Schweizerische Eidgenossenschaft
Confédération suisse
Confederazione Svizzera
Confederaziun svizra

Federal Department of the Environment, Transport,
Energy and Communications DETEC

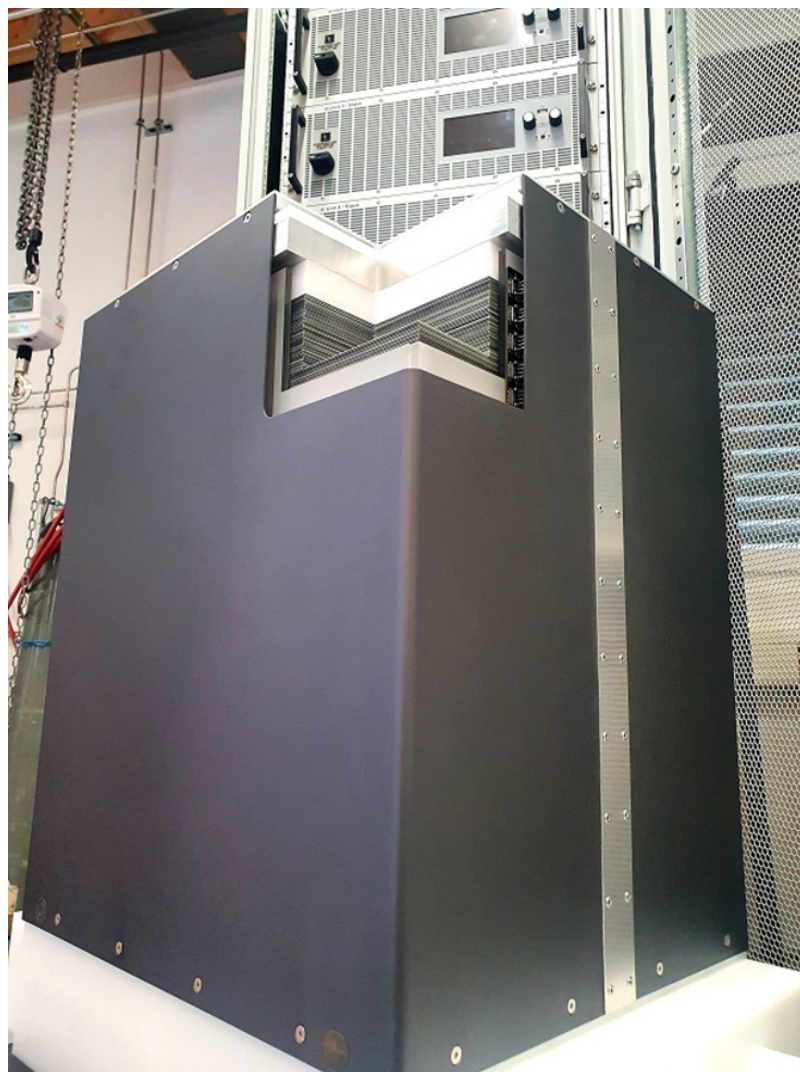**Swiss Federal Office of Energy SFOE**
Energy Research and Cleantech

Final report

EHSTACK-XL

Large single stack PEM Fuel Cell System for heavy duty mobility & large-scale stationary

Date: 20 March 2024

Location: Nyon

Authors:
Mardit Matian, EH Group Engineering AG, mardit.matian@ehgroup.ch
Christopher Brandon, EH Group Engineering AG, christopher.brandon@ehgroup.ch

In collaboration with EPFL (Jan Van Herle, Fuel Cell Group....)

The authors bear the entire responsibility for the content of this report and for the conclusions drawn therefrom.

Zusammenfassung

Ziel dieses Projekts ist die Untersuchung und Entwicklung eines grösseren PEM-Brennstoffzellensystems mit einer Leistung von bis zu 250 kW unter Verwendung einer neuen Plattform mit einem einzigen Brennstoffzellenstapel (EH-M87). Dies beinhaltete die Skalierung unseres Brennstoffzellenstapels durch die Verbesserung der MPL/GDL-Zellenkomponente (MPL = Microporous layer, GDL = Gas diffusion layer) und die Anpassung der übrigen Anlagenkomponenten (Befeuchter, Kompressor...). Im Ergebnis wird unser Brennstoffzellensystem kompakter und effizienter sein und niedrigere Herstellungskosten haben, da die doppelte Ausführung von Brennstoffzellen- und BoP-Komponenten entfällt. Der daraus resultierende Brennstoffzellensstack eignet sich für vielfältige Anwendungen, die von Mobilitätslösungen wie Lastwagen und Zügen bis hin zur Notstromversorgung für Rechenzentren oder Energiespeicher reichen.

Die Stapelbox entspricht der Produktnorm IEC 62282 und gewährleistet die Einhaltung von unter anderem Schifffahrtsvorschriften und EU-Anforderungen für stationäre Anwendungen. Sie weist Neigungsoszillationsfähigkeiten von bis zu ±30 Grad auf, sowohl statisch als auch in dynamischen Hin- und Herbewegungsszenarien. Die Stapelbox ist für Vibrationen bis 4g und Stösse bis 10g ausgelegt. Darüber hinaus bietet sie Schutz gegen das Eindringen von Wasser und Staub gemäß IP67-Norm und erfüllt die Anforderungen zur elektromagnetischer Verträglichkeit (EMC) hinsichtlich Störfestigkeit und Emissionen. Ausserdem verfügt sie über eine interne Belüftung, wobei die Belüftungsöffnungen strategisch ausserhalb des Gehäuses platziert sind, um Bedenken hinsichtlich einer möglichen Freisetzung oder Ansammlung von Wasserstoff innerhalb des Gehäuses auszuräumen. Dieses Design erfüllt verschiedene Standards, einschließlich der ATEX-Brand- und Explosionsanforderungen und der UL94-Entflammbarkeitsnorm.

Die Technologie wird im Einklang mit der weltweit anerkannten Norm IEC 62282 entwickelt, die bei der Entwicklung der Brennstoffzellentechnologie für verschiedene Anwendungen wie Automobile, stationäre Maschinen und den maritimen Einsatz weit verbreitet ist. Sie ist sowohl für die Nachrüstung bestehender Systeme als auch für die Implementierung in neue Anwendungen anpassbar.

Résumé

Ce projet vise à étudier et à améliorer un système de pile à combustible à membrane échangeuse de protons (PEM) plus grand, capable d'atteindre 250 kW grâce à la mise en œuvre d'une nouvelle plateforme de pile à combustible unique. L'effort consiste à améliorer la pile à combustible en affinant le composant de pile MPL/GDL et en ajustant les composants de l'équilibre de l'usine (tels que les humidificateurs et les compresseurs) pour s'aligner sur une pile unique. Cette approche conduit à un système de pile à combustible plus compact, efficace, évolutif et rentable, éliminant la duplication des composants de la pile à combustible et du reste de l'usine. L'élément constitutif de la pile à combustible qui en résulte démontre son adéquation à diverses applications, allant des solutions de mobilité telles que les camions et les trains à une alimentation de secours substantielle pour les centres de données ou le stockage d'énergie.

La boîte empilable est conforme à la norme de produit CEI 62282, garantissant ainsi la conformité aux réglementations maritimes, aux exigences des applications stationnaires de l'UE, etc. Il présente des capacités d'oscillation d'inclinaison jusqu'à ± 30 degrés, à la fois statiquement et dans des scénarios alternatifs dynamiques. La Stack Box est conçue pour résister à des vibrations jusqu'à 4g et à des chocs jusqu'à 10g. De plus, il offre une protection contre la pénétration d'eau et de poussière conformément aux normes IP67 et est conforme aux exigences CEM en matière d'immunité et d'émissions. Il intègre également une ventilation interne, avec des évents stratégiquement placés à l'extérieur de la boîte, répondant aux problèmes liés à la libération ou à l'accumulation potentielle d'hydrogène dans l'enceinte.

Cette conception répond à diverses normes, notamment les exigences ATEX en matière d'incendie et d'explosion et la norme d'inflammabilité UL94.

La technologie est développée conformément à la norme CEI 62282 mondialement reconnue, largement appliquée dans le développement de la technologie des piles à combustible pour diverses applications telles que l'automobile, les machines stationnaires et l'utilisation maritime. Il est adaptable à la fois pour la modernisation de systèmes existants et pour la mise en œuvre dans de nouvelles applications.

Summary

This project aims to investigate and enhance performance of a larger Proton Exchange Membrane (PEM) fuel cell system, capable of reaching +250 kW through the implementation of a novel single fuel cell stack platform. The endeavour involves upscaling the fuel cell stack performance by implementing several innovative steps based on EH Group's patented technology, reinventing the MPL/GDL structure and optimising performance and dimensioning of the balance-of-plant components (such as humidifiers and compressors). The new and innovative approach on MPL/GDL development (MPL = Microporous layer, GDL = Gas diffusion layer) assists in reduction of cell thickness, resistivity, improvement of gas flow and performance of the stack. This approach leads to a more compact, efficient, scalable, and cost-effective fuel cell system, eliminating the duplication of fuel cell stack and a few of the balance-of-plant components. The resulting fuel cell building block demonstrates suitability for diverse applications, ranging from mobility solutions like trucks and trains to substantial power backup for data centres or energy storage.

The MPL/GDL development involves

- Two types of uniform MPL/GDL layers for PEMFC have been developed.

- Improved structures are investigated in detail and compared to conventional materials.

- MPL/GDL Type I shows good electrical conductivity, low contact resistance, high porosity, and average thickness

- MPL/GDL Type II displays uniform pores and better apparent electrical conductivity, permeability, and diffusivity than existing manufactured material.

- Both types of developed MPL/GDL can improve mass transport, reduce ohmic losses, and achieve better water management.

The newly proposed innovation on MPL/GDL development and the stack design could be an optimal way for the industry to adapt. That includes development of larger stack platforms, faster production, higher reliability and better performance and lifetime.

Furthermore, the stack box design adheres to the IEC 62282 product standard, ensuring compliance with various applications such as maritime, aviation and stationary application requirements. It exhibits inclination oscillation capabilities up to ±30 degrees, both statically and in dynamic reciprocating scenarios. The stack box is designed to withstand vibrations up to 5g and shocks up to 10g. Moreover, it provides protection against water and dust ingress in accordance with IP67 norms and complies with EMC requirements for immunity and emissions. Also, it incorporates internal ventilation, with vents strategically placed outside the box, addressing concerns related to potential hydrogen release or accumulation within the enclosure. This design meets various standards, including fire and explosion requirements and the UL94 flammability standard.

As a result of this valuable collaboration with SFOE, we have developed a novel GDL/MPL that can be integrated into stack development for better performance. The new design and approach can be integrated in the next generation of production machinery that accelerate the deployment of EH Group fuel cell products to decarbonise large stationary power, aviation, and marine applications.

Contents

Abbreviations

PEMFC	Proton exchange membrane fuel cell
MPL	Microporous layer
GDL	Gas diffusion layer
BPP	Bipolar plate
BoP	Balance of plant
FC	Fuel cell
EMC	Electromagnetic compatibility
ATEX	Atmospheric explosive
OEM	Original equipment manufacturer
PTFE	Polytetrafluoroethylene
SEM	Scanning electron microscopy
EDX	Energy dispersive X-Ray
CT	Computational tomography
LBM	Lattice Boltzmann modelling
MRT	Multiple relaxation-time
P&ID	Piping and instrumentation diagram
GT	Gamma technologies
HT	High temperature
LT	Low temperature
CC	Cold cycle
ECU	Electronic control unit
PLC	Programable logic controller
HBV	High voltage box
HMI	Human-machine interface
CVM	Cell voltage monitoring
OCV	Open circuit voltage
STASHH	Standard sized heavy-duty hydrogen
CNC	Computer numerical control
ABPV	Air back pressure valve
I.D.	Internal diameter
RPM	Revolutions per minute
SFOE	Swiss Federal Office of Energy
PFSA	Perfluoro sulfonic acid
HRM	Hydrogen recirculation module
PWM	Pulse width modulation
NSD	Normal shut down

1   Introduction

1.1   Background information and current situation

Fuel cells and hydrogen technology have the potential to reduce global emissions and are considered the most suitable energy conversion device and energy source to overcome climate change and energy shortages. Among all the infrastructure challenges and device improvements that fuel cells must overcome in the next years, one of the most critical challenges is efficiency in production.

Mass production and ramp-up has been one of the main challenges of existing fuel cell developers. For larger power outputs (ex. MW scale), they have been using several stacks of 100 kW, which implies bulkier systems, duplication of components, and lower fuel efficiency. This is mainly due to limitations of the technology in the existing market.

EH Group is developing a single 250-300 kW stack platform technology that reduces production complexity and time. As a result, it simplifies the design of the balance of plant (BoP) components, without compromising the performance of the stack and the system. It is estimated that only the development of MPL/GDL will contribute about 10% towards the improvement of fuel cell power density [1]. We have been working and doing research in this area and have developed several prototypes in collaboration with EPFL that will be continued in the near future.

Dimensioning and sizing of various components in the stack has been one of the main challenges of this project as well as additional parameters/boundaries, such as operating temperatures, pressure, and cell dimensions that we have successfully tackled.

1.2   Purpose of the project

At EH Group (EGH), we believe that hydrogen technologies can be pushed a step further with a new 250-300 kW stack platform. The newly developed stack will reach a peak power of +300 kW with the option of expanding it to higher power outputs, which makes it a unique product in the market. Its high energy density will allow to generate a significant amount of power in a reduced and compact package. The stack box will be designed to meet the compliance requirements of marine, stationary and other applications. Additionally, it will follow IP67 norms to protect it against water and dust contamination.

Other fuel cell manufacturers follow the standard stamping/hydroforming approach in the production of stainless-steel bipolar plates. The main challenge and disadvantage of such an approach is limitation on miniaturising the gas channels dimensions – the technology allows production of gas channels where the width of the ribs (contact point between the plate and the gas diffusion layer (GDL)) can be reduced to 0.4 mm. The width of the channel where the gases flow is around 0.5 mm. With these dimensions the velocity of gas in the channels can reach to 50-80 m/s. One of the main disadvantages of this approach is that the large channel dimensions cause poor water/gas management, decrease the electrical and thermal conductivity between the layers, and accelerate corrosion rate on the contact surface between the GDL and the metal. In order to minimise corrosion of the metallic plate, protective coating is applied on the stamped plates [2]. However, most of the water accumulates in the ribs, which in its turn accelerates degradation rate of the cells.

EHG has a different approach for the production of metallic bipolar plates, which is simpler and easier; furthermore, it can assure excellent coating with minimum defects. A high corrosion resistance enables stable operation even under harsh conditions in fuel cells. The width of the gas flow channels is reduced to 0.1-0.22 mm and the width of the rib to 0.15-0.2 mm. This configuration allows a reduced gas velocity, and less accumulation of condensed water on the ribs. Furthermore, smaller gas channels assist in reducing thickness of the cells to less than 0.9 mm; hence, higher volumetric power density on the fuel cell stack. Also, the structure of the GDL/MPL (MPL = microporous layer) in combination of the innova-

tive gas flow channels enhance the performance and water/gas management in the cells. The separation of liquid/gas from each other is simplified, especially during load modulations, and delivery of hydrogen and oxygen to the catalyst is accelerated. Another advantage of EHG patented technology is an innovative and homogeneous way of delivering fresh gases to the active area. This potentially allows us to make the cell active area larger without compromising performance or manufacturing tolerance.

One of the main focuses of this project is the optimisation of the GDL/MPL and the development of an advance method for production, which is reproducible at large scale. Our bipolar plate (BPP) configuration allows good water management with a reduce GDL/MPL thickness. Available GDL products in the market are delivered at thickness from 180 to 400 µm. We believe that our stacks can efficiently perform with thickness less than 100 µm. The pathways for reactant gases (hydrogen and oxygen) are shortened by combination of our gas flow channels structure and reduction of GDL thickness, leading to improved mass transport within the fuel cell.

This reduction in diffusion distance enhances the efficiency of gas supply and facilitates quicker reaction rates at the catalyst layer. As a result, the overall electrochemical performance of the cell is improved, leading to higher power output and increased energy conversion efficiency. Additionally, the diminished thickness contributes to a reduction in mass and volume of the fuel cell, making it more compact and lightweight, thereby enhancing its suitability for various applications, including portable devices and automotive systems. In summary, the optimisation of GDL thickness represents a key strategy in enhancing the operational efficiency and practicality of the technology, offering benefits in terms of performance, size, and weight. Furthermore, there will be activities on reducing contact resistance between the GDL/MPL and the gas flow channels, which will be elaborated more in the following sections.

Performance of the GDL will be characterised and the main points to be evaluated are resistivity, electrical contact resistance, thermal/electrical conductivity, thickness, and porosity. The innovative techniques used and developed at EPFL, such as SEM/EDX (SEM = Scanning Electron Microscopy, EDX = Energy-dispersive X-ray spectroscopy) and CT (computed tomography) scan and Lattice Boltzmann modelling will allow us to investigate the structure of the carbon material and to identify the best physical features and properties for our application. For scaling up and mass production of the material, we have been in contact with several specialised suppliers in Switzerland, the most experienced one in the field is TSE Coating who will assist us in the next stages of development.

1.3 Objectives

The aim of this project is to design and prototype a single stack platform with larger active area up to 600 cm^2 using our innovative bipolar plate, flow field and GDL/MPL concepts that overcomes the limitations of the conventional approach. One of the main focusses is optimisation of the MPL/GDL structure, which implies the development and implementation of a method for larger scale production.

The research results from this project will allow the fuel cell development community to consider and deploy more efficient means of production in their commercialisation roadmap. In addition, original equipment manufacturers (OEMs), system integrators, and utility providers, will benefit from the opportunity provided to develop and integrate larger scale fuel cell systems into existing and new product offerings. Furthermore, we will be looking at integrating this new approach in our fuel cell production machinery (next generation) that is being built with our engineering partner based in St. Gallen.

This report is organised in two differentiated sections. The following Section 2. "Procedures and methodology" list all the techniques used to evaluate the performance of the MPL/GDL, as well as the tools for the design, dimensioning and dynamics of the stack and the system. It also describes the electrical network employed and the control codes that are needed to run the system.

2 Procedures and methodology

2.1 Combination of microporous layer (MPL) and gas diffusion layer (GDL)

In this study, the fabrication of MPL/GDL made from the slurry of polytetrafluoroethylene (PTFE) mixed with carbon black is investigated in detail. The microstructure of the developed GDL containing MPL is analysed by scanning electron microscopy (SEM) observing the surface of the specimen. The properties, such as electric conductivity, thickness and porosity are measured.

2.1.1 Preparation of MPL/GDL

The MPL layer is made from a solution of water as solvent, triton as surfactant, and an aqueous polymer resin (PTFE) added to carbon powder followed by mixing at high speed for several hours. The carbon slurry is then coated on a carbon substrate (GDL) using a screen-printing machine, followed by drying thermally at 380°C to form the MPL microstructure.

2.1.2 Electrical properties

In-plane electrical resistance was measured using the method reported by Williams *et al.* [3]. The resistance was measured at 10 mm increments on GDL samples cut 100 mm x 2 mm. The measured resistance (R) values were plotted against distances (l) and yielded a linear relationship whereby the slope of the line represented the in-plane resistance per unit of distance (R').

The *in-plane* resistivity (R') values were calculated using Ohm's Law following Eq. 1.

$$\text{Eq. 1} \qquad R = (R'\, l)/A \rightarrow R' = RA/l$$

where, R is the resistance of the GDL in Ω, R' is the *in-plane* resistivity in Ω m, A is the cross-sectional area of the GDL sample in m^2 and l is the length of the GDL sample in m.

Interfacial contact resistance between gas diffusion layers and bipolar plates was measured following a technique proposed by Wang et al [4] with a setup designed in-house (Figure 1). A bipolar plate is used to simulate our fuel cells. The GDL samples were placed between two bipolar plates and then between two copper plates as electrodes, connected to a voltage divider circuit. The copper plates were cleaned before every test with sandpaper to avoid the formation of surface oxides that cause errors. Then, a current (increasing from 0.1 A to 1 A by steps of 0.1 A) was passed through the two copper plates, and the voltage difference between the two ends of the electrodes was measured by a multimeter (DAQ970A station). The measured potential difference was used to calculate the total resistance (R_T) of the setup. The applied pressure is maintained at 1MPa.

Two different setups were used to calculate the contact resistance of the bipolar plates with the GDL (Figure 1). The total resistance (R_{T1}) after applying the compaction force of 1MPa and measuring using a data acquisition system can be summarized as follow in Eq. 2:

$$\text{Eq. 2} \qquad R_{T1} = 2R_{Cu} + 2R_{Cu-BP} + R_{GDL} + 2R_{BP-GDL} + 2R_{BP} + R_i,$$

where R_{Cu} is the resistance of the two copper plates, R_{GDL} is the resistance of the GDL and R_{BP}, of the bipolar plates, R_{Cu-BP} and R_{BP-GDL} are the contact resistance between the copper plates and the bipolar plates and the bipolar plates and the GDL, respectively. R_i is the internal resistance due to wires, and power supply, etc.

The total resistance in the second setup is given in Eq. 3.

$$\text{Eq. 3} \qquad R_{T2} = 2R_{Cu} + 2R_{Cu-BP} + 1R_{BP} + R_i$$

By subtracting Eq. 2 from Eq. 1, the contact resistance of the bipolar plate with the GDL, R_{BP-GDL} can be determined, Eq. 4. R_{GDL} and R_{BP} are neglected due to their small values.

$$\text{Eq. 4} \qquad R_{BP-GDL} = 0.5\,(R_{T1} - R_{T2} - R_{BP} + R_{GDL}) \approx 0.5\,(R_{T1} - R_{T2})$$
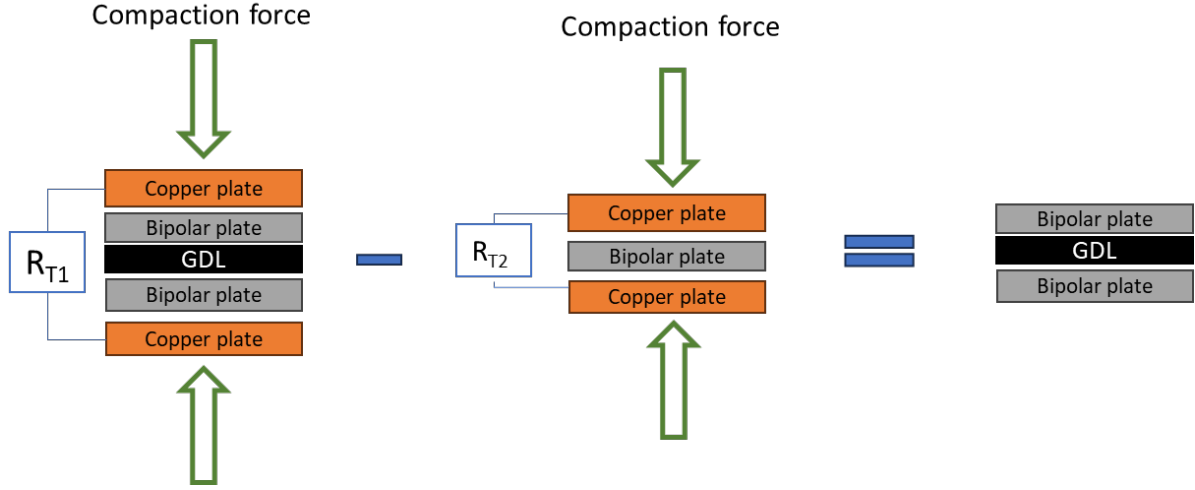
Figure 1. Schematic representation of the measurements performed, reproduced from [5].

2.1.3 Scanning Electron Microscopy (SEM) and Energy Dispersive X-Ray (EDX)

Scanning Electron Microscopy (SEM) is a powerful tool to characterize surfaces as it allows both the morphology and composition of materials to be investigated. It is considered a relatively rapid, inexpensive, and basically non-destructive approach to surface analysis. Energy Dispersive X-Ray (EDX) spectroscopy is applied along with SEM to analyse the types and the quantity of elements at the surface or vicinity of the surface of the GDL.

2.1.4 Computational tomography (CT) scan and Lattice Boltzmann modelling (LBM)

Computational tomography (CT) scan is also a non-destructive technique and one of the best options to obtain the structure of the porous region of gas diffusion layers considering the thickness, which is approximately between 150-400 µm. SEM can measure up to a resolution of 3 nm, while CT scan reaches 1 µm. The combination of CT scan, which provides the geometry of the GDL, accompanied by the Lattice Boltzmann modelling, LBM computational fluid dynamic simulation enables the quantitative measurement of water breakthroughs inside the GDL.

The GDL geometry presented in this work has been obtained using µ−CT scan imaging with the operating conditions indicated in Table 1.

Table 1. Operating conditions to perform CT scan and characteristic of the analyzed GDL samples.

Parameter	Value	Parameter	Value
Acceleration voltage	40 kV	Averaging frames	10
Current	120 µA	Exposure time	500 ms
Image resolution	1 µm	Rotation step	0.22 degrees
Sample size (X-direction)	1.685 mm	Sample size (Y-direction)	1.464 mm
Sample size (Z-direction)	0.225 mm	Stage temperature	21°C
Voxel size (X-direction)	1685	Voxel size (Y-direction)	1464
Voxel size (Z-direction)	225		

To implement the Multiple Relaxation-Time (MRT) model, the LBM can be developed based on the MRT collosion equation considering the force term as of Eq. 5.

$$\text{Eq. 5} \qquad f(x + e\Delta t, t + \Delta t) = f(x,t) - M^{-1}[SM(f^{eq}(x,t)) + \left(l - \frac{1}{2}S\right)MF]$$

here, the density distribution function is shown with f, while Δt is the time step. M indicates the orthogonal matrix, which transfers the distribution functions and S is the diagonal matrix designed. F represents the body forces based on the Guo's model [6].

Avizo software, provided license by PIXE at EPFL, and Dragonfly software, are used for the segmentation and reconstruction of the GDL images.

2.2   250 kW-stack and -system

The design of a new stack platform consists in optimising the internal structure, sizes, spacings, and thickness of single cells and external shape, as volume and weight of the stack, so that the total resistance of the system is minimised and the net power is maximised. The gained experience optimising these parameters in our stacks over the years allows us to confidently scale up our stack platform to next level, 250 kW.

This section explains design of the process, as well as building and control of the system that will enable complex and innovative stack tests.

2.2.1   System and component design and simulations based on large stack platform

The first step in the design of the BoP is to know the characteristics of the stack to which the BoP will be implemented. The process is an iterative cycle that consist in 6 phases. The design starts by defining the initial required functionalities, and the type of components, which are configured and connected in a certain way. This must be done for all the subsystems. Fuel cell systems mostly consists of four submodules: (1) a hydrogen fuel delivery system which delivers hydrogen fuel to the stack at the appropriate flow and pressure; (2) an air delivery system for safe and efficient operation of PEM fuel cells; (3) a thermal management system to guarantees the hydration of the polymeric membrane and the condition of the catalyst; (4) and an electrical power supply system to connect or isolate the fuel cell stack from the load.

Depending on the availability of the components in the market, adjustments to the initial layout are made. In some cases, components have been developed in-house because the ones commercially available did not fulfil our requirements. The development of these in-house components becomes a project on its own and about 80% of the design must be achieved before the 3D concept can be completed and 100% of the design concluded before the 3D detailed phase can be completed. Once the 3D detailed phase is 100% completed, the procurement and assembly start, which end with the commissioning of the test bench. SolidWorks, MATLAB and Inkscape are the software used for the design of the test bench.

0D/1D simulations help to identify, analyse, and optimise bottle necks in dimensioning of stacks and systems. It enables the user (integrators and customers) to optimise for control and tune the system for the most efficient operating conditions. In addition, it allows to obtain information about process for internal usage and for customer requirements. The procedure is an iterative process which contains more information about the fuel cell and/or the system with each iteration.

The procedure for 0D/1D simulations is:

- Defining the flow paths (anode, cathode, cooling) and the fuel cell characteristics.
- Integrate third party or in-house designed components and have the components separately calibrated in the software tool.
- Implementing desired P&ID control.
- Investigate flow conditions, component performance, and control to pinpoint bottle necks.

The multi-physics platform Gamma Technologies (GT) is used to perform 0D/1D simulations. The simulation methodology is divided in four separate parts: cathode, anode, cooling, and fuel cell.

Cathode: supplies the conditioned air for a PEMFC of 125 kW. Two identical cathode loops will provide the conditioned air for 250 kW system. With respect to computational time the cathode loop is made only once.

Anode: supplies hydrogen to the PEMFC of 125 kW from two sources, a hydrogen source and recirculated hydrogen. The anode loop is made only in once computational time, as the second anode loop is identical to the first one. Both will supply the required hydrogen for a 250 kW PEMFC.

Cooling: consists of 4 closed loops: 2 high temperature (HT) coolant loops to cool down the 250 kW PEMFC, 1 low temperature (LT) coolant loop to cool the compressor, inverter, and intercooler, and 1 cold cycle (CC) coolant loop that transports the heat from the 3 previously mentioned loops to the building. A single HT coolant loop can dissipate ~130 kW of heat. In order to mimic the heat dissipation of a 250 kW stack, the heat rejection from the HT coolant loop to the CC coolant loop is multiplied by 2. This helps to reduce the computational time. The same reasoning is used for the LT Coolant loop and the CC coolant loop.

Fuel Cell characteristics: are based on experimental data of the EH M81 platform. GT uses 3 stages of calibration to achieve high accuracy for the fuel cell. During the simulation, the model demands a user defined current from the fuel cell. The Electronic Control Unit (ECU) controls the various components to achieve the predefined desired operation conditions.

2.2.2   Electrics and Electronics

A robust electrical network capable of handling many sensors and actuators is needed for the 250 kW system. The system must work within a harsh environment without compromising its integrity. Programable Logic Controller (PLC) is the control unit used to enhance modularity and flexibility for adding and replacing sensors and actuators if needed.

The electrical part of the system consists of 4 elements: BoP, High Voltage Box (HVB), control panel, and power signal distribution.

The BoP refers to the collection of systems and equipment that support the main process (solenoid valves, pressure, or temperature sensors) excluding the primary power generation unit. The HVB serves as a central enclosure that houses several high-voltage equipment and components, such as circuit breakers and protective devices. It plays a vital role in managing and distributing voltage coming out from the fuel cell safely and efficiently. The primary purpose of the control panel is to regulate, monitor and manage electrical processes and equipment. housing a set of electrical devices, switches, and control components (PLC, relays, contactors, circuit breakers, etc.).

The power/signal distribution refers to the network of electrical circuits and communication channels responsible for delivering power, data, and control signals to the BoP. The distribution network consists of power supplies, capacitors, switch gears and wiring systems, ensuring that the right amount of electricity reaches each destination reliably and safely.

The recirculated current, I in the AC network is given by Eq. 6.

$$\text{Eq. 6} \qquad\qquad I = \frac{P}{\sqrt{3}*V_{line}*PF}$$

where V_{line} is the line voltage and PF the power factor. In order recirculate a current of 365 A, an upgrade of the EHG electrical installation was conducted by a third party in our facilities.

The process for selecting the sensors and actuators is carried out between the different teams to ensure integration compatibility. Power consumption, electrical signal range, signal type, and temperature of operation are some considerations for validating the electrical and electronics BoP compatibility.

2.2.3   Control

The control team's objective is to develop an accessible and secure interface that enables users to conduct experiments on various sizes of fuel cells with ease and safety. The experiments aim to characterise the fuel cell properties, explore new concepts, and optimise membrane activation under favourable conditions. Due to the dynamic nature of the environment driven by extensive research and development on the prototype, it is imperative for the team to design a control system that is easily updatable and must:

- Provide human-machine interface (HMI).

- Provide a control structure that simplifies the user decisions.

- Design a control framework that is easy to update and easy to use.

- Implement and run experimental test and validation protocols at all stages of the project.

- Support the other engineering teams.

MATLAB, Simulink development environments and tools on those platforms are used to create a four core components software that controls the system. The controllers and the supervisory system development are in Simulink and reuse the experience gained over the last four years. The embedded support for the codes is TwinCAT – A Beckhoff platform that enables the use of Simulink codes. The HMI and the data post-processing are a MATLAB App. Since these four coding environments have to be updated each time sensors and actuators are moved, replaced, added, etc, a "master code" has been developed to set up all the interactions between them and always guarantee correct data sharing.

3 Results and discussion

3.1 MPL/GDL

3.1.1 Developments and properties

The primary purpose of the MPL/GDL within the fuel cell is to conduct electrons and heat, while maintaining the mechanical integrity of the membrane electrode assembly and allow gas diffusivity while removing the water toward the flow channels. Giving the characteristics of our unique flow channels, a thin layer of MPL will be sufficient to guarantee the reactant gas diffusion and water control and this is where our effort is focussed.

Ohmic losses in PEMFC occur due to the resistance of materials (also known as resistivity) and the interfacial contact resistance between the electrochemical active area, the gas diffusion layer and current collector materials. Such losses must be reduced to maximize the conversion of chemical energy to electricity rather than heat.

The resistance of the materials within PEMFC can vary depending on several factors, including the specific materials used, their thickness, and their conductivity properties. The membrane resistance has decreased as manufacturing improvements have led to the development of thinner membranes, thus decreasing the membrane geometric area over thickness. For the same reason, EH Group has focused in redefining the GDL/MPL design followed by thinner GDL to decrease its resistivity.

Nevertheless, the resistivity of the materials themselves (such as the membrane, gas diffusion layers, electrodes, and current collectors) is lower compared to the interfacial contact resistance between layers, particularly at the boundary between the BPP and GDL. The interface between the BPP and GDL involves a relatively small contact area, especially at the microscopic level where surface roughness can come into play. Even if the materials themselves have low resistance, any imperfections or gaps at this interface can significantly increase resistance.

In the development of MPL/GDL during this project we have successfully reduced the thickness of the MPL/GDL while maintaining the resistivity and interfacial contact resistance values comparable to commercial materials. We have dedicated special attention to the surface roughness as bulk materials with good conductivity, that shows surface irregularities can create barriers to electron transfer.

Although the MPL/GDL synthetic procedure is straightforward, converting scientific findings into industrial technology applications is still a major challenge. First, the characteristics of materials alter when scaled up, just as they do when downscaled to the nanoscale; specifically, the amount of control that can be exercised at the nanometre scale diminish at macro scales. In conventional materials most of the atoms are not at a surface, they form the bulk of the material. While bulk materials have constant physical properties regardless of size, the size of the carbon nanoparticles in the formation of the MPL/GDL dictates its physical and chemical properties, and this has major impacts on the porosity and morphology of the films.

One of the main issues observed while scaling up the MPL/GDL are the visible cracks and pores on the surface of the microporous layer formed during the deposition process. The particles size of the carbon nanoparticles (carbon black) used for making MPL usually goes from 18-50 nm. Different sizes of the precursor material give rise different average porous size on the final material. Despite the impact and mechanism of cracks in MPL on water management are still unclear [7], this can be minimised by using a larger carbon size particle. Whereas, if the powder size of carbon is too small, the final material will show an average pore size very small. Thus, the access of fuel and a reaction gas to a catalyst layer may be inhibited, and discharge of potentially carbon dioxide and water produced during reaction may not be efficiently performed [8].

A literature review was carried out to gain understanding on the best material composition and concentration, advantages of different experimental protocols and instrumental approach (Schematic representation of the research can be seen at Appendix 1). Following Latorrata *et al.* [8], Tanaka *et al.* [9], and Shrestha *et al.* [10], three synthetic routes for MPL/GDL were attempted. However, it was decided to incorporate some of the useful aspects of those papers and to work on a new design with new means of production in-house, leveraging our own protocol based on previous experience. As a result, two different procedures were conducted to produce two MPL/GDLs with different properties.

MPL/GDL Type I

The preliminary results were satisfactory, as we were able to produce uniform layers without major issues, as shown in Figure 2 (a). SEM and CT scan were used to investigate the structure, pore sizes, and thickness of the MPL. Although cracks were not perceived by eye, SEM images of the surface showed the presence of some cracks at micrometre scale, Figure 2 (b). SEM analysis of commercially available GDL from major manufacturers, such as Sigracet SGL (22BB) and Freudenberg (H14C10), as well as literature research were carried out for comparison (Figure 2 (c) and (d), respectively). The MPL surface from Freudenberg is highly porous and cracks-free, while the one provided from SGL exhibits some cracks. Same cracks were found in the literature for GDL from same provider SGL, as show in Figure 2 (e-f) [11].

An ongoing debate of the scientific community anticipates that cracks in the MPL are advantageous as they can facilitate removal of liquid water from the catalyst layer and consequently improve the durability of the platinum. However, too many cracks can result in poor contact between the MPL and the MEA [12, 13].
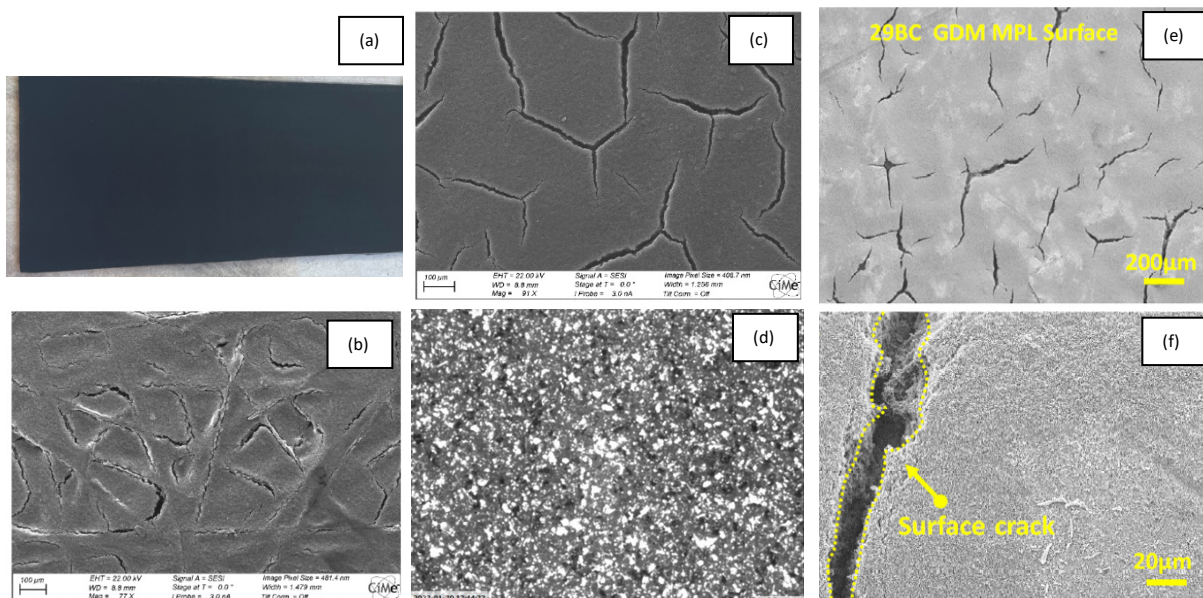

Figure 2. (a) Picture of GDL produced at EHG, and SEM images of (b) EHG GDL sample, (c) Sigracet SGL (22BB), (d) Freudenberg (H14C10) and (e-f) SGL sample taken from [11].

The thickness and morphology of MPL/GDL plays an influential role in the overall performance of the fuel cell. It is shown that the combination of thin gas diffusion layer (thickness~100 μm) and high flow field open area fractions can facilitate water removal/oxygen supply from/to the catalyst layer and can provide a more uniform oxygen distribution over large cell active areas [14]. Porosity, thickness, and electrical properties results for six samples prepared in our lab are compared with commercial GDL Freudenberg (H14C10) in Table 2 and Figure 3. The thickness of most commercial GDLs is usually

among 180-400 µm. The thickness achieved of our samples (~100 µm) and similar porosity to the commercial one (~55%) make our GDLs good candidates to meet the above requirements. It can be seen that the average pore diameter does not decrease with decreasing thickness.

With the increase in compressive stress in a cell, the thickness gradually decreased and became thinner and thinner. However, porosity does not decrease considerably. The change in porosity observed for our samples after compression was around 3-5%, which might be due to inaccuracies during the segmentation and reconstruction of the images. It is estimated that differences up to 5% in CT scan measurement can be neglected due to uncertainties in the method.

Table 2. Thickness, porosity data and electrical properties for various MPL/GDL

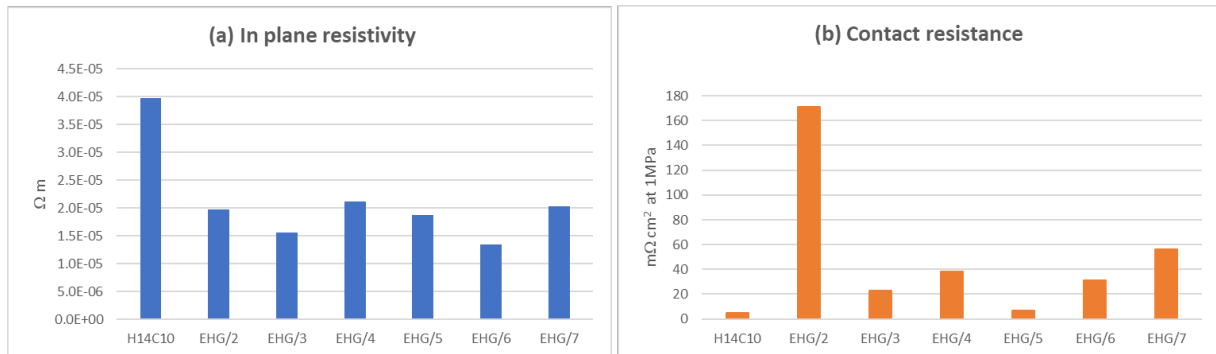| Sample	Porosity	Thickness		In plane resistivity	Contact resistance
		MPL	GDL		
	%	µm		Ω m	mΩ cm^2 at 1MPa
H14C10	55.42	40	120	4.0E-05	5
EHG/2	58.64	30	130	2.0E-05	171
EHG/3	59.60	60	100	1.6E-05	23
EHG/4	55.60	50	80	2.1E-05	38
EHG/5	55.37	40	110	1.9E-05	7
EHG/6	55.17	60	100	1.4E-05	31
EHG/7	55.89	60	100	2.0E-05	56

Figure 3. In-plane resistivity (a) and contact electrical resistance (b) of GDL materials.

The electrical performance of GDLs is commonly stated by in-plane resistivity which is the material's inherent characteristic. Anisotropy in the in-plane electrical resistivity of GDLs is greatly determined by carbon fibre orientation in the porous layer. The results show low values of resistivity, around 1.7×10^{-5} Ωm. These values are consistent with literature for commercialized GDLs [15]. The decrease trend in the in-plane electrical resistance (or resistivity) of the six GDLs respect to H14C10 as observed in Figure 3 (a) is probably due to the good connectivity among carbon fibres, as high interconnection between the fibres facilitates the flow of electrons through the GDL.

In a fuel cell, the critical parameter for good performance is the interfacial contact resistance between the main components: bipolar plate, MPL/GDL, and catalyst layer. Moreover, the main purpose of the MPL is to minimize the contact resistance between the GDL and the catalyst layer. Connectivity between

carbon fibres increases as compressive loads increase, as electrical contact resistance decreases. This means that the electrical conductivity of the GDL changes with the assembly force in the fuel cell and is highly dependent on the pressure applied. Also, it is important to consider that compression has irreversible effect on the GDL due to material deformation. Figure 3 (b) shows the GDL contact resistance at 1 MPa clamping pressure. The figure shows similar values for EHG/5 and H14C10 of 7 and 5 mΩ cm^2, respectively. The contact resistance of the H14C10, provided by Freudenberg match the values of commercial GDLs found in the literature [15]. EHG/2 exhibits a very high resistance that might be related to the small MPL thickness and considerably large GDL respect to the others. In addition, minor imperfections were spotted on the surface. The resistance of the rest of the GDL samples is within the expected range.

MPL/GDL Type II

In general terms, lowering the thickness of the MPL/GDL in combination with our innovative flow channels results in better performance of the stack since it increases the speed of reactants to reach the catalysts. However, the main obstacle is the formation of ultra-thin and at the same time highly porous GDL, without compromising its high thermal and electrical conductivity. We have shown above that slightly reducing the MPL thickness is beneficial, and bulk porosity is not affected. It must be emphasized the fact that not only the amount of porous structure is important, but also its distribution is crucial and has to be controlled for large scale commercialization.
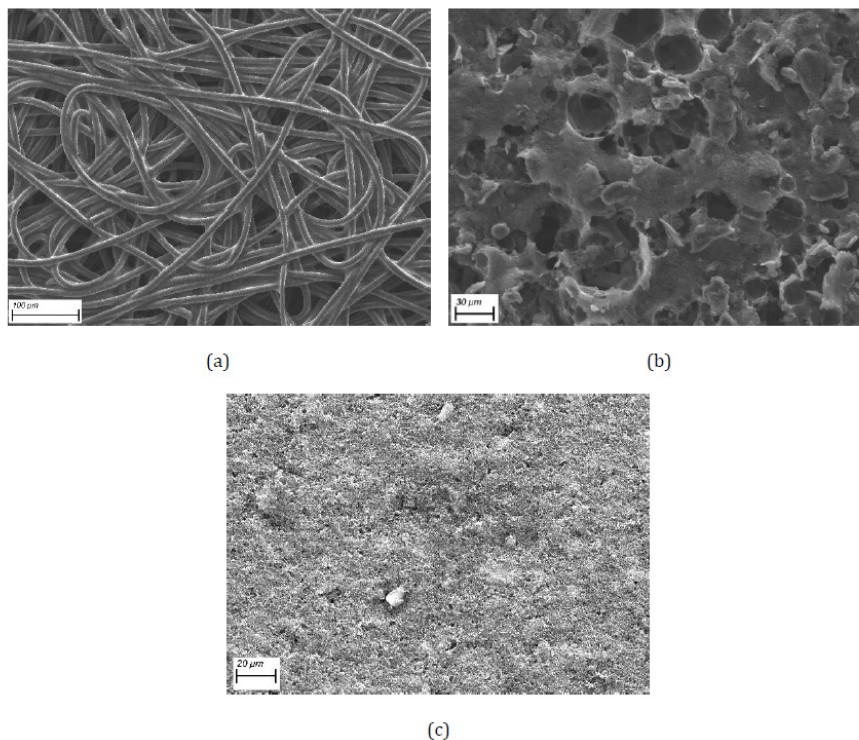

(a)

(b)

(c)

Figure 4. The obtained SEM images of the reference commercial sample on the GDL (a and b) both sides. SEM image of the in-house GDL (c). Images have been obtained on the working distance of 6.6 mm with the electron high tension of 22 kV to facilitate the EDX analysis while the probe's current density was 3 nA.

While the benefit of GDLs with cracks as water removal pathways is clearly established, an alternative method was carried out to produce thinner (below 100 µm) and cracks-free GDL. The method enables the production of thinner material without any defects with uniform porosity throughout the sample. The

measurements on conductivity, permeability, and other microstructural properties also verified the quality of the GDL. Results will be explained in comparison to the commercial sample of Freudenberg H14C10, as in type I.

Figure 4 shows the obtained SEM images of the H14C10 and the prepared in-house GDL. As can be seen the surface morphology of our GDL is homogenous and has small pores that enable the transport of the reactants and the removal of the liquid water. The size of the pores is smaller (maximum 2 µm see Figure 4 (c)) than the H14C10 (around 50 µm see Figure 4 (a) and (b)). Smaller size pore enables lower velocities of the reactants and might decrease the formation of water columns inside the GDL. The formation of the water columns inside the GDL is considered a deteriorating phenomenon since it degrades the pores faster and increases the possibility of ice formation in sub-zero temperatures that lead to difficulties for cold start. Regarding the velocities, lower velocities due to smaller pore size is compensated by the extremely low thickness of our sample (28.9 µm in comparison to 170 µm of H14C10). To sum up, our material shows low size, and homogeneously distributed pores in 1/5 of the thickness of commercial GDL.

From SEM/EDX images, it is possible to calculate the electrical conductivity, s, of the samples through their chemical composition, Table 3. Conductivity of our sample is found $\sigma = 1.2 \times 10^3$ S/m, compared to 1.5×10^3 S/m of H14C10.

Table 3. EDX composition for in-house GDL and commercial sample, H14C10.

Element	In-house GDL (wt%)	H14C10 (wt%)
Carbon	63.1	78.4
Oxygen	10.1	5.1
Fluorine	25.4	16.4
Potassium	0.07	0.02
Nickel	0.79	0
Copper	0.5	0.2

A second protocol was followed to improve the structure of the MPL/GDL type II by increasing the PTFE concentration. Although the uniformity of the films was improved compared to the previous method, a slightly increase in contact resistance values was observed. Latest MPL prepared and characterised at our lab of 50 µm showed an average contact resistance of 35 mΩ cm^2 at 1MPa.

The contact resistance at the interface between the bipolar plate and the GDL is the main contribution to the total electrical resistance of the fuel cell. Thus, the characteristics of the surface of these two materials (BPP and GDL) play an important role in the electrical conductivity, thermal management and overall performance of the stack. The measurement of the surface roughness is used here to evaluate these materials. If the surface roughness of the materials is smooth, the contact between the BPP and the MPL is uniform decreasing the electrical resistance. Whereas, if it is rough, the would be a poor contact and high electrical resistance to the flow of electrons.

Surface roughness of two samples, EHG/8 and EHG/9 were measured at the Centre of MicroNano-Technology at EPFL (Figure 5). The image of the surface roughness for EHG/8, in Figure 5 (a), shows a 2.5 µm thick defect on the centre of the surface visible in the profile scan. The average distance to mean surface for this sample, S_a is 0.223 µm. Such variations in surface roughness led to an uneven

contact resistance of 35 mΩ cm^2 at 1 MPa, which can result in localized hot spots, decreased performance, and potential mechanical failure. Image for EHG/9 surface roughness is shown in Figure 5 (b). Well defined structures of parallel lines are observed for this sample. Lines of S_a=0.23 µm comprise most of the surface roughness features. Profile X for EHG/9 showed some valleys of approx. 0.5 µm, but overall, it is more homogeneous than EHG/8, which agrees with the measured contact resistance of 3 mΩ cm^2 at 1 MPa.

Common values for this type of material are between 1 and 10 microns. Surface roughness also affects the compression behaviour of the stack. Bipolar plates are typically compressed together within the stack to ensure good electrical contact. S_a of around 0.2 µm allows a good control of compression forces, ensuring proper sealing without excessive deformation or damage to the bipolar plates. The results and data show the significant impact of the surface topography on the contact resistance of composite bipolar plate/GDL interface.
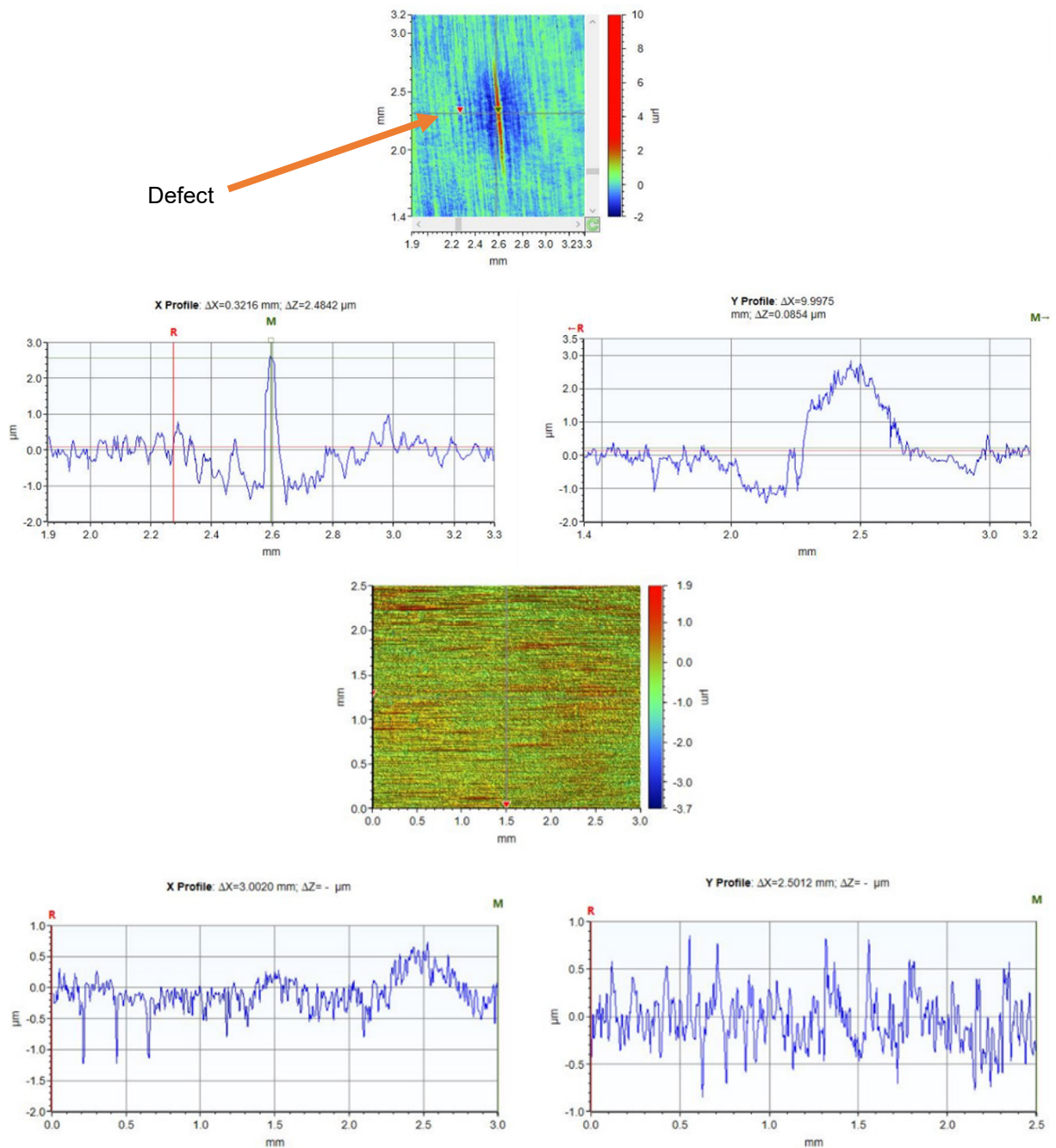
Figure 5. Surface roughness microscopic images and two profile scans (in x and y directions) for (a) EHG/8 where a surface defect can be spotted and (b) EHG/9 where the surface is smooth.

Surface roughness is quantified by the deviations in the direction of the normal vector of a real surface from its ideal form. If the deviations are large, as seen in sample EHG/10 in Figure 6 (a), the surface is rough; if they are small, the surface is smooth (sample EHG/11). A rough surface has a lot of irregularities and is more sensitive to friction and would cause higher contact resistance.
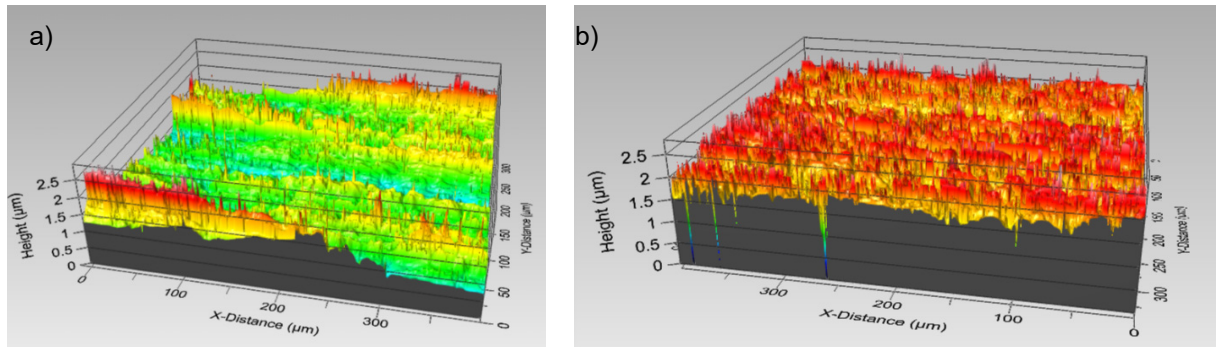
Figure 6. Surface roughness microscopic images for two samples: (a) EHG/10, where the surface is not homogenous and colour mapping changes as of differences in roughness, and (b) EHG/11, and homogeneous sample.

3.1.2 CT scan and Lattice Boltzmann modelling

Figure 7 (a) and (b) illustrate the results of the reconstructed images for H14C10 and in-house GDL, respectively. H14C10 reconstruction in Figure 7 (a) shows three well-distinguished regions, carbon fibre (blue), PTFE binder (red), and pores (white). Figure 7 (b) illustrates the thin GDL by solid (light red) and pores (white) phases. By governing equations, the microstructural properties can be calculated using the Avizo and Dragonfly software. Table 4 shows the results of the microstructural analysis obtained by the Xlab Simulation module by Avizo and the calculated porosity/thickness by the Dragonfly software.
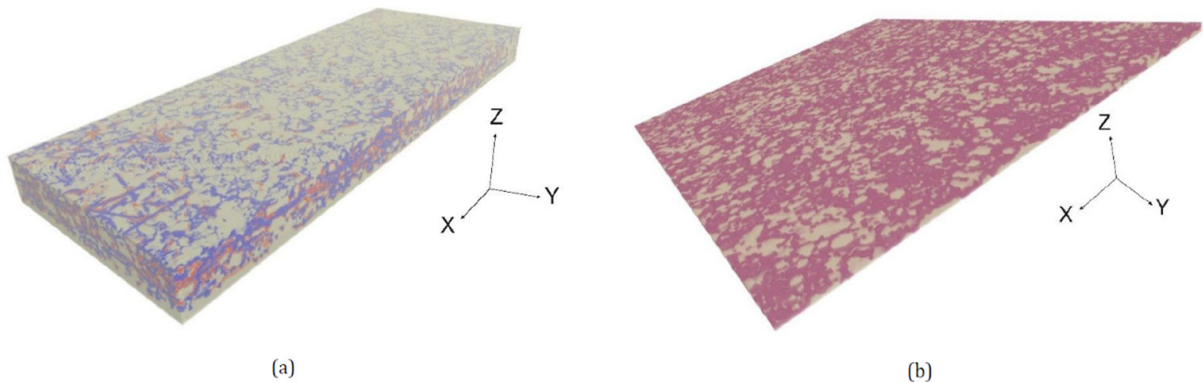

Figure 7. The segmented and reconstructed images of the reference commercial sample (a) and the in-house GDL sample (b).

Table 4. The microstructural properties obtained by Avizo software and the reconstructed geometry.

Microstructural parameter	In-house GDL	H14C10
Porosity (%)	44.7 - 46.1	62.2 - 63.1
Thickness (µm)	28.5 - 29.3	167.5 - 172.5
Absolute permeability (μm^2)	2453 - 2527	38.1 - 39.2
Absolute permeability (d)	2485 - 2561	38.6 - 39.8
Apparent electrical conductivity (S/m)	1527 - 1573	1166 - 1201
Apparent formation factor	3.7 - 3.8	1.8 - 1.9
Input concentration (mol/m^3)	1685 - 1736	1685 - 1736
Output concentration (mol/m^3)	0	0
Apparent molecular diffusivity (m^2/s)	0.047 - 0.049	0.038 - 0.040
Apparent thermal conductivity (W/mK)	10 - 10.3	15.3 - 15.8

The results of the microstructural properties indicate that the developed GDL has better electrical conductivity, molecular diffusivity, and absolute permeability than the commercial one. However, it exhibits lower thermal conductivity. A recent publication carried out by Büchi *and coworkers* [16], studied the role and optimum values of the GDL's thermal conductivity and if it is a decisive factor for water management. Results show that lower GDL thermal conductivity produces higher temperature gradients in the GDL, which are, however, partially compensated by a heat pipe cooling mechanism. This suggested that thermal conductivity should not be a decisive criterion for future materials developments of optimized GDLs to improve fuel cell performance at high current densities, but rather the GDL structure.

H14C10 is a known and proved efficient MPL/GDL material for water/thermal management within fuel cells. The outstanding structural features of our material, such as lower pore size and homogeneously distributed pores, compared to H14C10, make it a good candidate to provide high performances in fuel cells. The MPL/GDL layer prepared has a dimension of 10 x 30 cm, scalability of the product, while maintaining the physical properties still need to be confirmed.

3.2 Stacks

3.2.1 Small stack prototype: Design and Test

The design of the stack in Figure 8 (a) is based on previous experience on EH 51 platform. With this configuration, it is possible to achieve up to 15 kW. One of the main advantages of the current design is that it is scalable; hence, the active area of the cell can be extended to 200-500 cm^2 or beyond without compromising the performance. Furthermore, the end plates, current collectors and also protective cover around the stack are designed to be compatible with the automotive and certification standards (IP67 rated). A new and improved in-house designed CVM (Cell Voltage Monitoring) unit is added to the stack in order to measure voltage of individual cells during operation. This device allows us to diagnose the state of the whole stack in real time, monitoring the voltage of each cell at a rate of 1 ms. Figure 8 (b) shows an image of EH M51 model, 45 cells, and 5 KW.
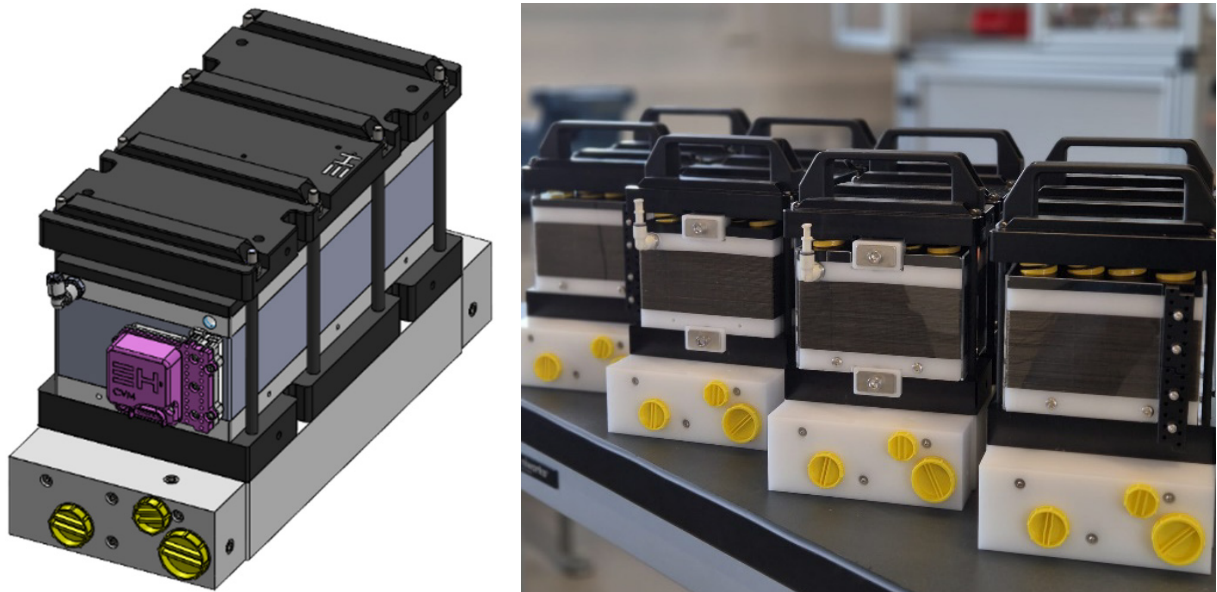
Figure 8. EH M51 fuel cell of 45 cells, and 5 kW. (a) CAD model (b) assembled stacks.

An example of the IV curve of these stacks is shown in Figure 9. Reliable voltage/current data requires a stable environment, where the temperature, pressure, humidity, and flow rates are maintained during the test. This stack was tested at constant temperature of 65 °C and different cathode pressure of 1.4-2.5 bar. The relative humidity (RH%) was kept at 70-75%. Hydrogen and air flow was maintained at a stoichiometry of 1.6, and 2.1, respectively.
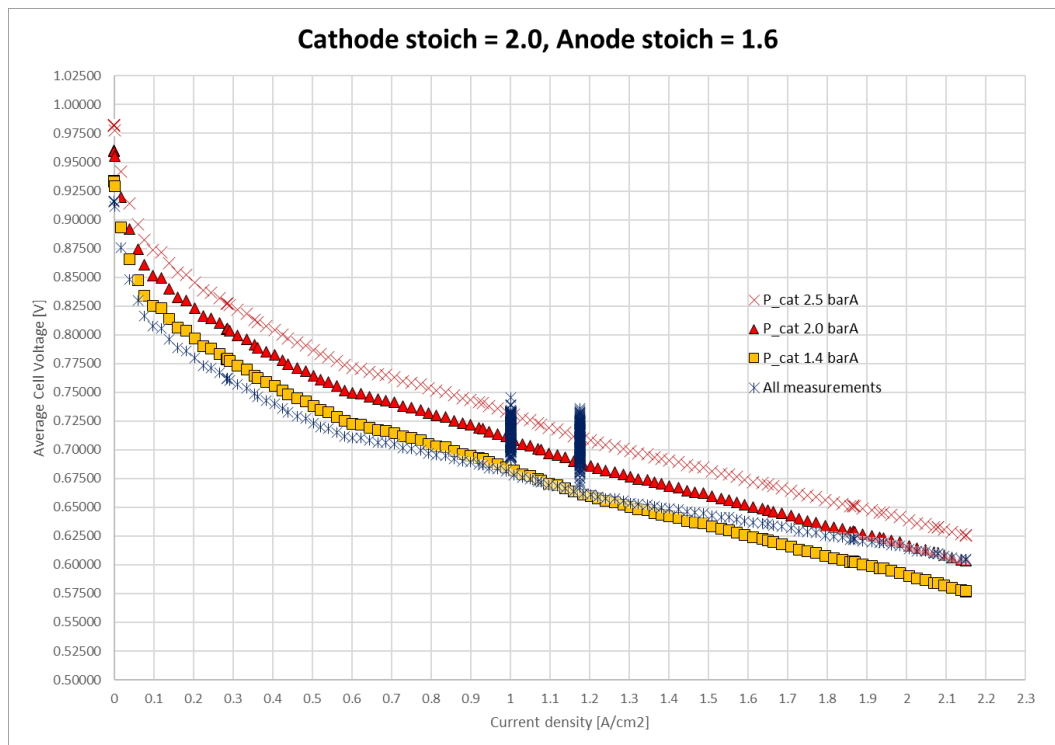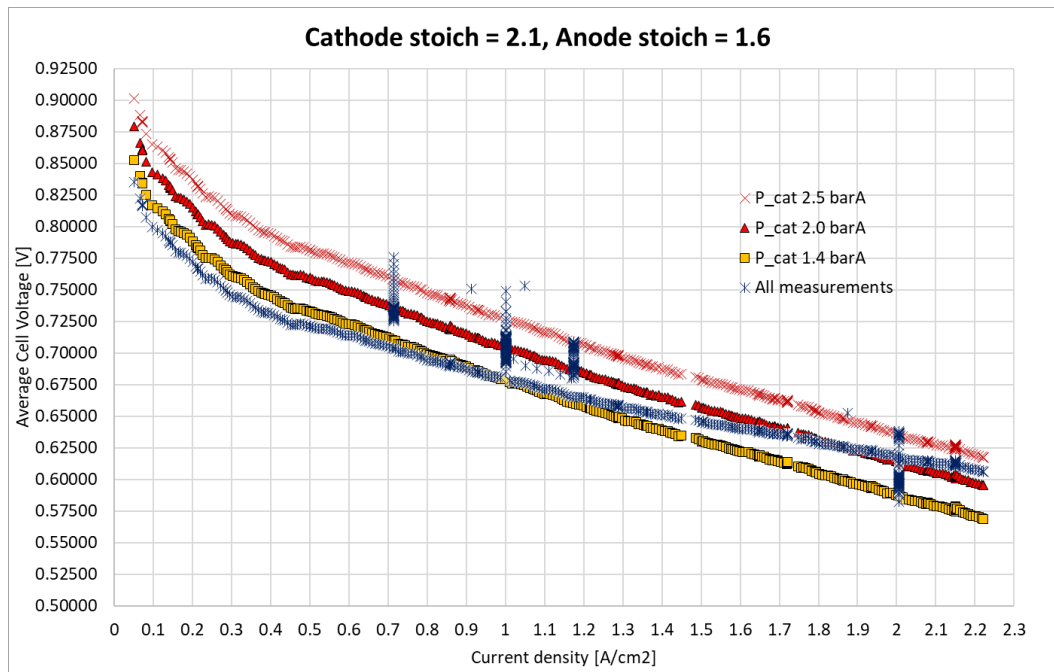
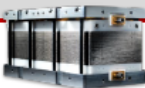Figure 9. IV curves for 2 stacks EH M51 new generation.

3.2.2   Large stack (200-250 kW)

As stated, the goal of the project is to develop fuel cell modules for large and heavy-duty applications with standardised interfaces, control, and test protocols, with the objective of kickstarting the use of fuel cells and hydrogen in the heavy-duty mobility sector, where electrification with batteries is impractical. Multiple modules must be integrated in a system, similar to batteries; this will allow using the same modules for multiple sizes. Combined with the standardisation across several sectors (road, offroad, rail, maritime, etc.) represented by participating OEMs, the same modules will address a large pooled market.

The first step in the project development is to standardise the size of a single fuel cell platform to satisfy customer needs for mobility and stationary applications. This is proposed by the norms being established at the European level by the STASHH standard. Specifications of the stack proposed by EHG for the current project is depicted in Table 5.

Table 5. FC proposed specifications

EH Fuel Cell Stacks

	Power [kW]	Voltage Range [V]	Current Range [A]	Dimensions [mm]	Weight * [kg]
EH - 31					
	1	8 - 15		280 x 90 x 98	~ 4
	2.5	16 - 32	0 - 180	280 x 90 x 110	~ 5.5
	4	24 - 48		280 x 90 x 130	~ 7.5
EH - 51					
	5	19 - 39		280 x 120 x 190	~ 13
	10	36 - 72	0 - 320	280 x 120 x 230	~ 18
	15	52 - 105		280 x 120 x 290	~ 24
EH - 81					
	20	47 - 94		400 x 120 x 260	~ 32
	40	94 - 187		400 x 120 x 320	~ 48
	60	140 - 281	0 - 450	400 x 120 x 450	~ 64
	80	187 - 374		400 x 120 x 530	~ 80
	100	231 - 462		400 x 120 x 610	~ 96
EH - 87					
	150	140 - 281 or 280 - 562	0 - 1000	400 x 330 x 250	~ 61
	200	184 - 369 or 368 - 738	or	400 x 330 x 310	~ 77
	250	231 - 462 or 462 - 924	0 - 600	400 x 330 x 380	~ 96

|	EH - 31	EH - 51	EH - 81	EH - 87
Operating Conditions - Cathode				
Quality	Filtered, no impurities			
Inlet Temperature [°C]	65 - 70			
Outet Temperature [°C]	76 - 80 (85 short run)			
RH [%] - No Condensation	35 - 80			
Stoichiometry [λ]	1.5 - 2.5			
Pressure Level [kPa g]	< 150			
Pressure Drop [kPa] (0.6 [V] operation)	< 60	< 30	< 40	< 35
Operating Conditions - Anode				
Quality	> 99.995 (SAE J2719 or ISO 14687:2019 grade D)			
Inlet Temperature [°C]	65 - 70			
RH [%] - No Condensation	< 40		20 - 80	
Stoichiometry [λ]	1.2 - 1.8			
Pressure Level [kPa g]	< 150			
Pressure Drop [kPa] (0.6 [V] operation)	< 25	< 20	< 35	
Operating Conditions - Coolant				
Quality	DI water, DI + anti - freeze			
Inlet Temperature [°C]	65 - 70			
ΔT [°C]	6 - 8		8 - 10	
Pressure Drop [kPa] @ 20 [°C]	< 60		< 100	
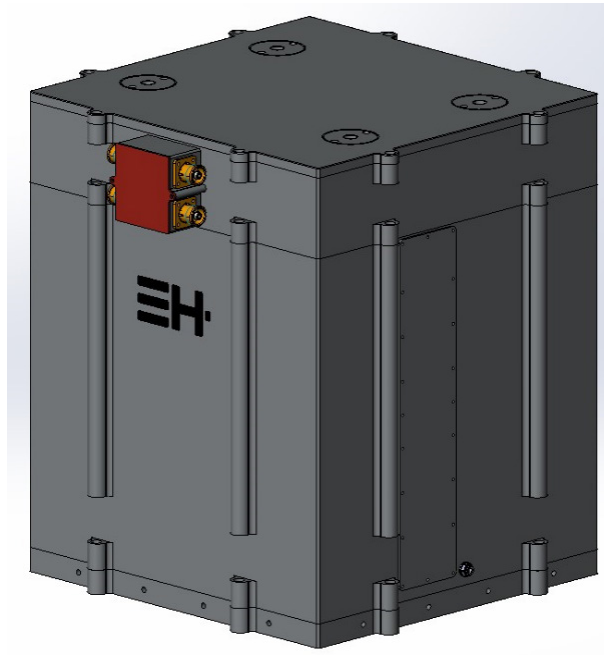
Figure 10. CAD configuration of EH M87 stack box.

Prototyping of the first cover around the stack is done by CNC machining, which is depicted in Figure 10. This gives us the greatest flexibility for minor design changes on our first FC power units.

The combination of "lost wax castings" and CNC machining for the manufacturing of the outer manifolds will allow more flexibility and cost reduction at this stage of development. Lost wax casting provides unique manufacturing advantages to create complex internal geometry of gas and liquid transporting channels that cannot be machined or require splitting the components into multiple pieces and assembled. This technology will be used to manufacture the inlet/outlet manifolds of the stack.

The stack box is designed to meet the compliance requirements of marine applications with inclination oscillation up to +/- 30 degrees and reciprocating 10 g testing. Additionally, our stack boxes are designed to protect against water and dust ingress to IP67 norms. A filtered air supply will be connected to the stack box, thus providing a purging gas flow evacuating any unintended buildup of hydrogen gas inside the stack box enclosure.

Our patented CVM solution will be housed inside the stack box, where we monitor cell voltages during operation.
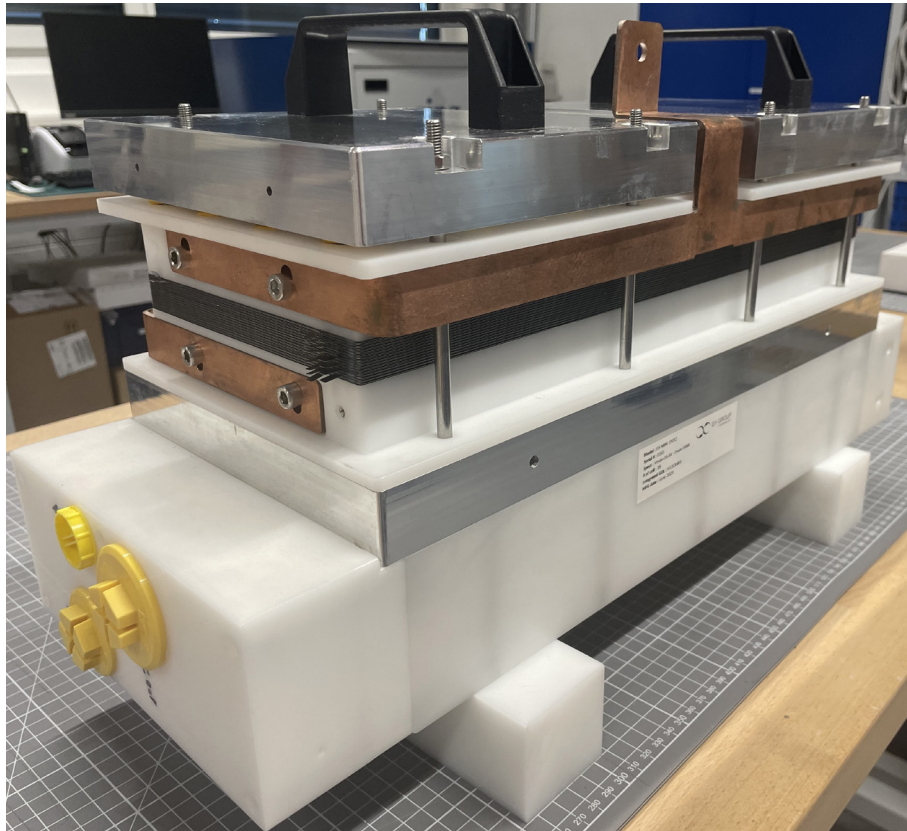
Figure 11. Image of first prototype of EH M87, 15 cells, and 5 kW.

Figure 11 shows the first prototype of EH M87 stack. Its compactness, lightweight and top handles allow easy integration in the systems. Experimental tests are currently being performed in this stack. The results of the simulations are shown in Figure 12. The characteristics used to run the simulations are based on a previous EH stack platform, 450 cells stack of EH 81. The graphs on the left depict the pressure drop at the cathode side of the fuel cell with respect to air velocity and air mass flow rate. The graphs on the right show the pressure drop over the anode side with respect to anode velocity and mass flow. The bottom graph illustrates the pressure drop of the coolant with respect to the coolant volume flow rate.
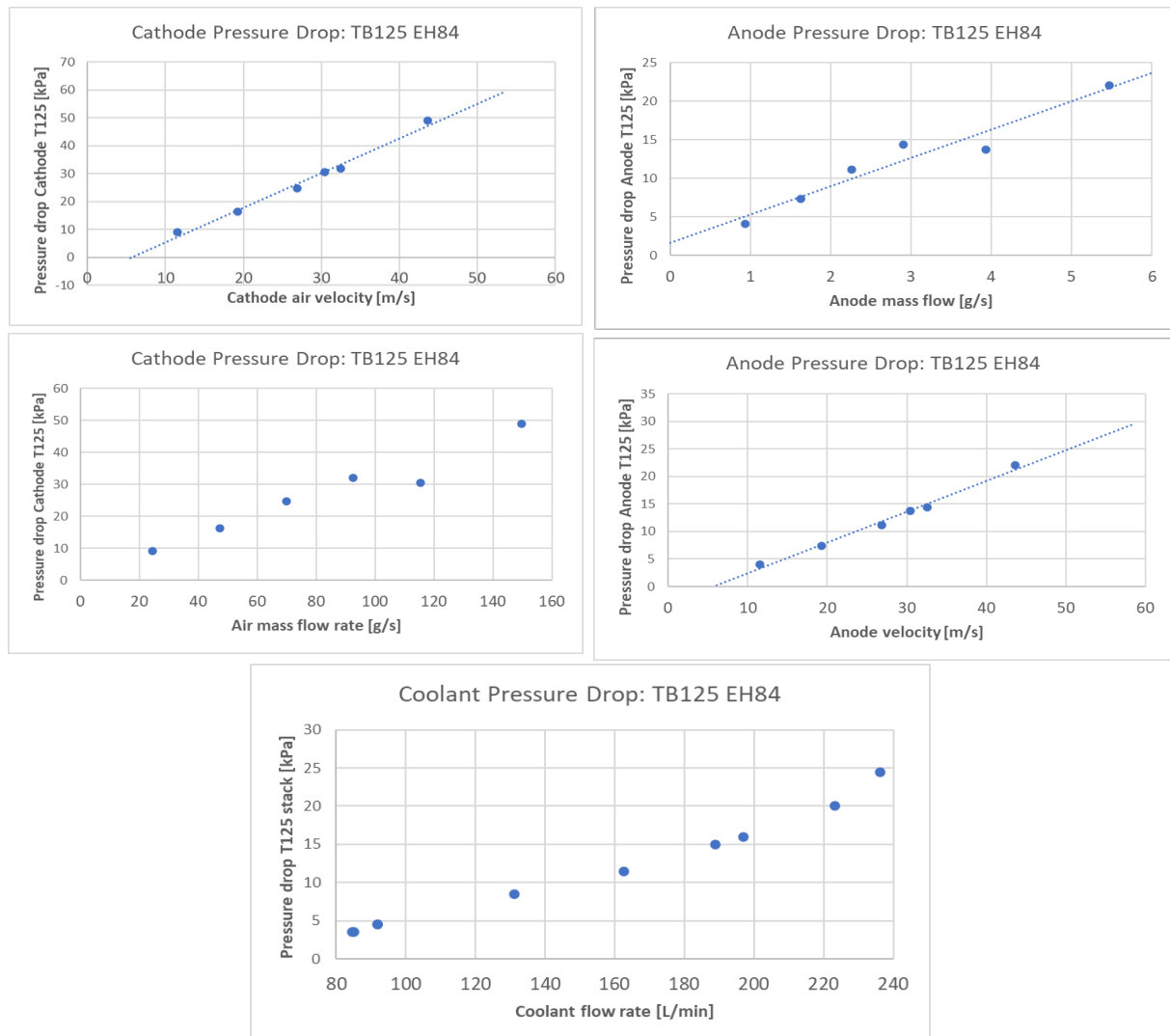
Figure 12. Calculated pressure drop for cathode, anode and coolant within the fuel cell.

3.3   250 kW-system

3.3.1   Structures and interfaces

State of the art fuel cell systems consist of four different sub-modules, which are easily spotted in the P&ID. Each of which must fulfil a specific need of the fuel cell stack.

The cathode sub-module provides oxygen from the air and the anode provides hydrogen. The chemical reaction of hydrogen and oxygen produces water, heat and electricity, which are taken care of by the cathode, cooling systems and the high voltage module, respectively. Each subsystem must create the correct thermodynamic state at the inlet and outlet of the stack for all the sub-modules. The relevant components on each subsystem control parameters like pressure, temperature, relative humidity, flow rate, conductivity, and chemical composition. In general, every parameter needs one actuator.

The main components in the cathode are the air filter, the compressor, the intercooler, the humidifier, and the air back pressure valve, ABPV.

Most fuel cells are developed in laboratories with relatively clean and ideal air conditions. However, real world applications, especially mobile deployments, are frequently in harsh environmental conditions

which present challenges regarding clean air delivery. Several filters were considered for our system and Figure 13 shows the average pressure drop for two of them. Freudenberg air filter has a pressure drop of 9.7 kPa at 158 g/s ambient air, which was selected for the project. A higher pressure drop over the air filter increases the pressure ratio in the compressor. A higher-pressure ratio results in higher air temperatures at the compressor outlet. The cooling duty of intercooler increases to reach the same target temperature at the fuel cell air inlet while also maintaining the same target pressure. A higher pressure drop over the air filter limits the compressor at higher air stoichiometries due to higher pressure ratio. Bigger air filter implies a filtration device that has less pressure resistance than the suggested FC-F-650-N. Reason for bigger air filter is less resistance experienced by the compressor and therefore less power required to operate the fuel cell system. However, the downside is that maintenance costs, bigger filters will increase the cost.
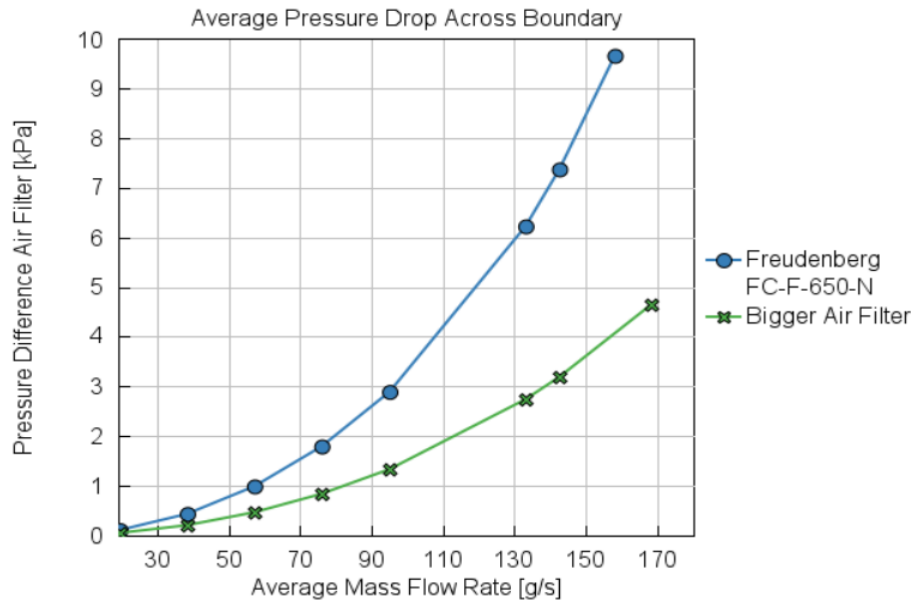

Figure 13. Average pressure drop across boundary for both air filters.

The speed and efficiency maps of one of the compressors under investigation can be seen in Figure 14 (a) and (b), respectively. The red line in Figure 14 (a) is the operating line when the air pressure back valve is fully open (44 mm I.D.). The region above the red line is the operating region for the compressor. The corrected mass flow rate indicated in the graphs above is not the real mass flow rate. The compressor map is shifted towards the left if the inlet pressure at the compressor becomes lower, see Eq. 7.

$$\text{Eq. 7} \qquad \dot{m}_{corrected} = \dot{m}_{actual} * \sqrt{\frac{T_{inlet\ total}}{298}} \Big/ \frac{P_{inlet\ total}}{100}$$

For example, the corrected mass flow at a pressure ratio of 2.32 is 178 g/s. However, the inlet pressure in the compressor is 0.84 barA, not 1 barA (100 kPa, in Eq. 7). Also, the inlet temperature in the compressor is 18.5 °C, not 25 °C (298 K). Both factors, P and T influence the actual mass flow. The actual mass flow in this scenario is 158 g/s at 1.0 barA and 25 °C ambient.

Higher pressure at the cathode fuel cell inlet will result in lower air mass flows. This will limit the possibility for higher power requests from the stack. To reduce the heat rejection from the compressor to the low temperature coolant loop the compressor must run more efficiently.
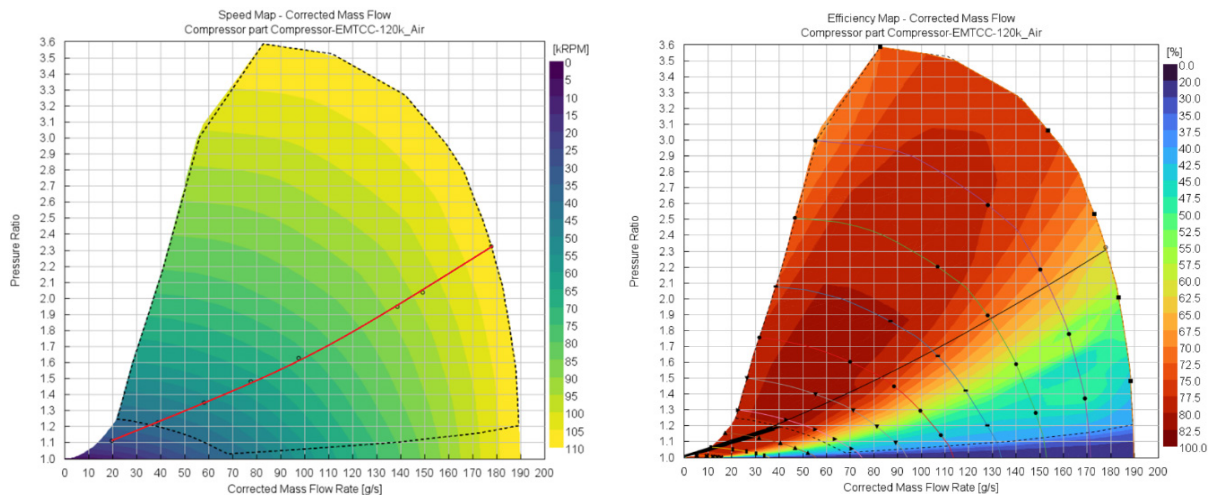
Figure 14. Fischer EMTCC-120k Air (a) Speed map and (b) Efficiency map.

An intercooler is a heat exchanger used to cool a gas after compression. The maximum pressure drop on the air side of the intercooler is 1.45 kPa and the actual air mass flow is 158 g/s (11300 l/min, ρ_{air} = 1.67 kg/m^3).

Cathode air must be humidified before supply to the anodes and cathodes in order to maintain high performance and to avoid dehydration of the membrane and ionomers. Simulations showed than the maximum pressure drop on the dry air side of the humidifier is 4 kPa at a real air mass flow of 158 g/s (4900 l/min, ρ_{air} = 2.05 kg/m^3). The maximum pressure drop on the wet air side is 6 kPa at a real air mass flow of 158 g/s (9500 L/min, ρ_{air} = 1.07 kg/m^3). The dewpoint temperature becomes lower at the cathode fuel cell inlet due to the higher flow velocity in the humidifier. Also, at higher air stoichiometries the air has less retention time in the fuel cell stack. This results in lower dewpoint temperatures at the cathode fuel cell outlet.

EHG systems have an anode recirculation loop to evenly distribute gas and improve fuel utilisation. There is a valve present in the exhaust line on the anode that is periodically opened in order to release inert gases. The hydrogen recirculation module, HRM consists of a fuel injection valve, the gas pre-heater and two ejectors.

In order to have design flexibility on the anode sub-module, EHG decided to design and standardised an ejector block internally.

As mentioned previously, 4 cooling loops are needed for the 250 kW system: 2 HT (high temperature) coolant loops to cool down the fuel cell stack, 1 LT (low temperature) coolant loop to cool the compressor, inverter, and intercooler, and 1 CC (cold cycle) coolant loop that transports the heat from the 4 previously mentioned loops to the building.

Each HT coolant loop must dissipate a rate of ~125 kW of heat. This means that components in the HT coolant cycle must operate at certain specific conditions. The coolant pump must have a minimum flow rate of 205 l/min through the fuel cell to maintain a temperature difference (ΔT) of 10 °C between the coolant fuel cell inlet and outlet. The minimum volume flow rate must be 3% of the maximum volume flow rate to minimize current leakage. The expansion tank has an internal volume of 2.6 litres and the total volume of expansion of the coolant liquid in the HT cycle is approximately 1.5 l (from 20 °C to 85 °C). The 3-way valve is fully opened when 125 kW of heat dissipation is reached (No bypass flow). All flow passes through the Liquid-To-Liquid Heat Exchanger, LTL HEX which can dissipate 250 kW of heat. The total volume of the HT cycle is ~13.73 litres and Tthe total pressure drop over the pipes is 24.6 kPa at 205 l/min.

The coolant pump flow for the LT cycle is ~128 l/min at maximum duty. Figure 15 shows the characteristic flow curve of the coolant pump in LT coolant loop.
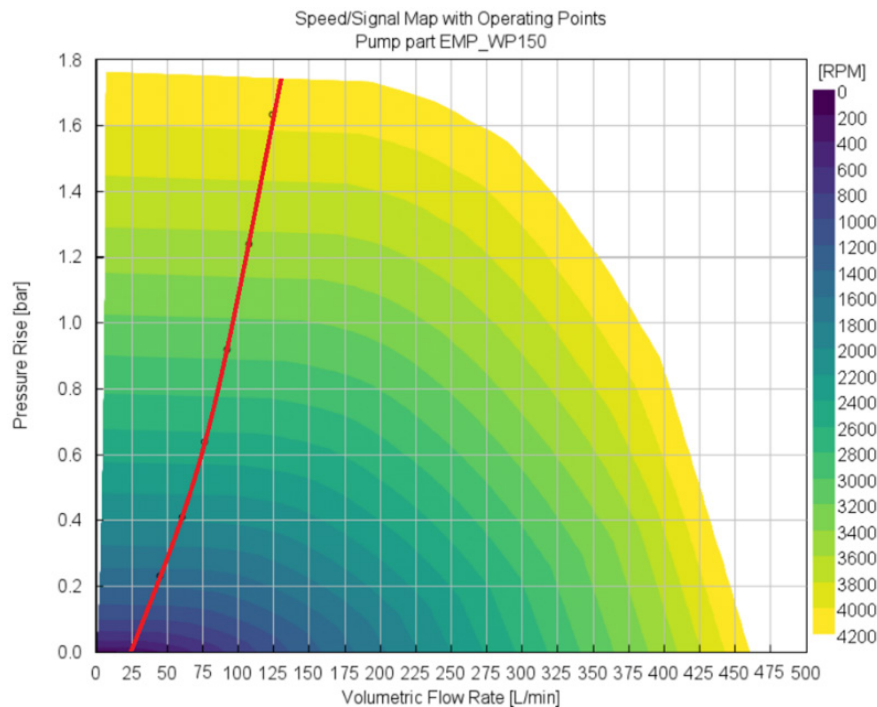

Figure 15. Characteristic flow curve of the EMP WP150 coolant pump in LT coolant loop.

The dual stage air compressor and inverter have a fixed heat rejection obtained by simulations of 2.5 kW and 1.25 kW, respectively. The LTL HEX can reject 55 kW before the hot (red line in Figure 15) side becomes limited in heat rejection. The total volume expansion in the LT cycle is approximately 0.41 litres (from 20°C to 60°C). The pressure drop is ~1.0 bar at 100 l/min. The maximum total heat rejection is 42.5 kW in the LT cycle.

The CC coolant loop collect the dissipated energy from the two HT coolant cycles and one LT coolant cycles. This results in a total heat dissipation of 305 kW that needs to be dissipated to a separate cooling loop. The coolant pump for the CC Loop must have a minimum volume flow rate of 340 l/min to effectively dissipate 305 kW of heat and maintain the desired temperatures in the LT and HT coolant loops. Two 250 kW LTL HEXs are used in the CC Coolant Loop: one cold side in which the minimum volume flow must be 240 l/min to transfer 250 kW of heat, and one hot side in which the minimum volume flow is 190 l/min to transfer 250 kW of heat.

The high voltage box is a component to guarantee a safe operation for personnel and the stack. The main parts are contactors (to break the line in case of emergency or after shut down), the diode (to prevent reverse current and therefore operating the stack as an electrolyzer), the dump resistor and contactor (to remove the residual voltage during the shutdown procedure), and a voltage and current sensor (to assist the already mentioned features and to validate if the system operating points corresponds to the power setpoint). The HVB was designed in-house, as the need of another liquid cooling system was required for the 250 kW system. Additional safety standards were included to better comply with certification.

Due to various technical and commercial constraints regarding sourcing and procurement of the components for the test bench, the final manufacturing and assembly of the test bench has been delayed.

3.3.2 Electronics & electrics

The 250 kW system design has around 120 sensors and actuators, including pressure, temperature, relative humidity sensors, mass flow meters, servo motors, solenoids, electronic throttle bodies, etc. to control all the components of the system safely. While the price of industrial PLC and I/O boards is slightly high compared to other solutions, such as automotive ECU (electronic control unit), it becomes quickly justified when we address robustness, ease of integration, and especially the capability of expanding and replacing the sensors and actuators within the system, as shown Figure 16. The advantage is that the system can be improved and modified along its life cycle without compromising its integrity. It is required to ensure that the sensors' and actuators signal types are chosen accordingly with the most available I/O types.

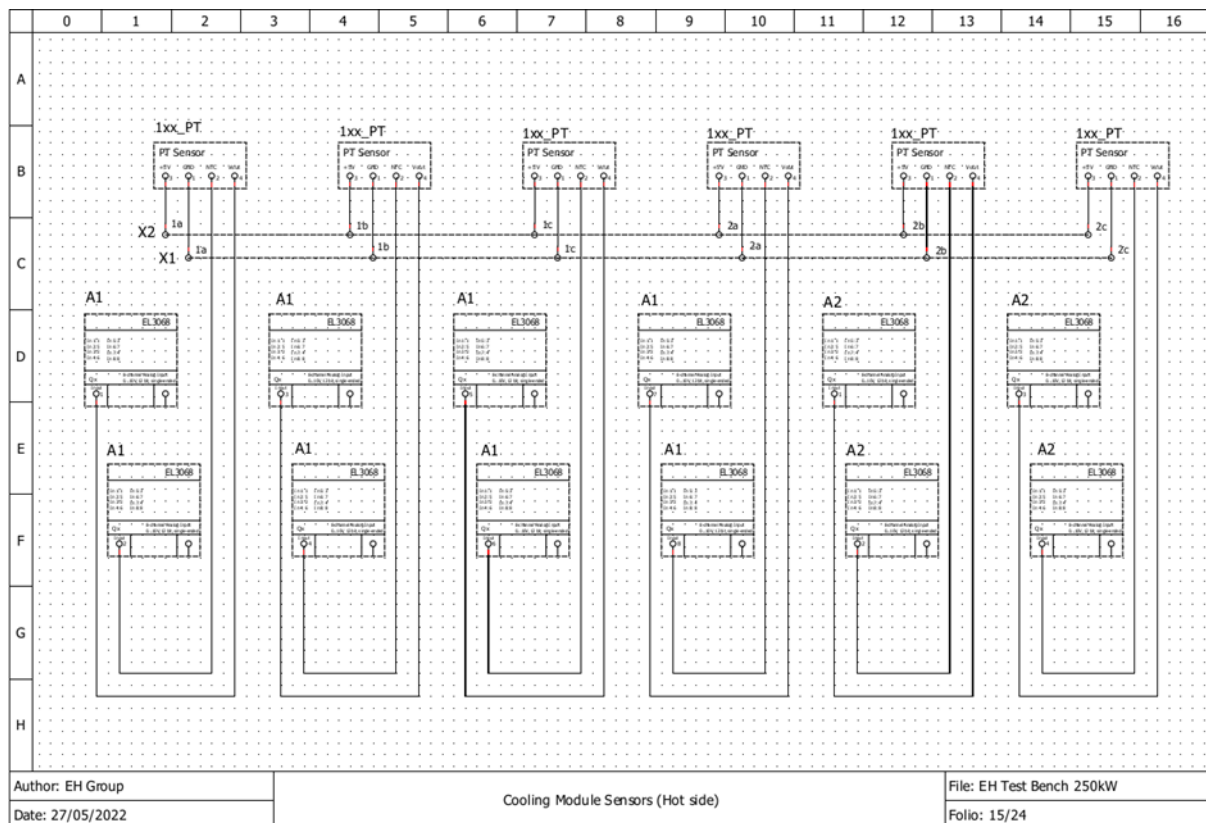Figure 16. Electrical diagram extract showing same types of sensors connected on different channels of the same terminal.

3.3.3 Control architecture

The control architecture for the 250kW system can be separated in four modules:

1. The master file

2. The industrial computer embedded on the system.

3. The control algorithms.

4. HMI. In the following section each of those modules are detailed.

1. The Master file: Since adaptability is a key feature of the design of control architectures, in particular in the context of the development of new systems which generally involves frequent updates, it is important to build it in such a way that update time and efforts are reduced as much as possible. To this end, the interfaces between all the modules that constitute the control system are managed by a "master file" that updates them with reference to the latest state of the system. Figure 17 illustrates the function of the master file.
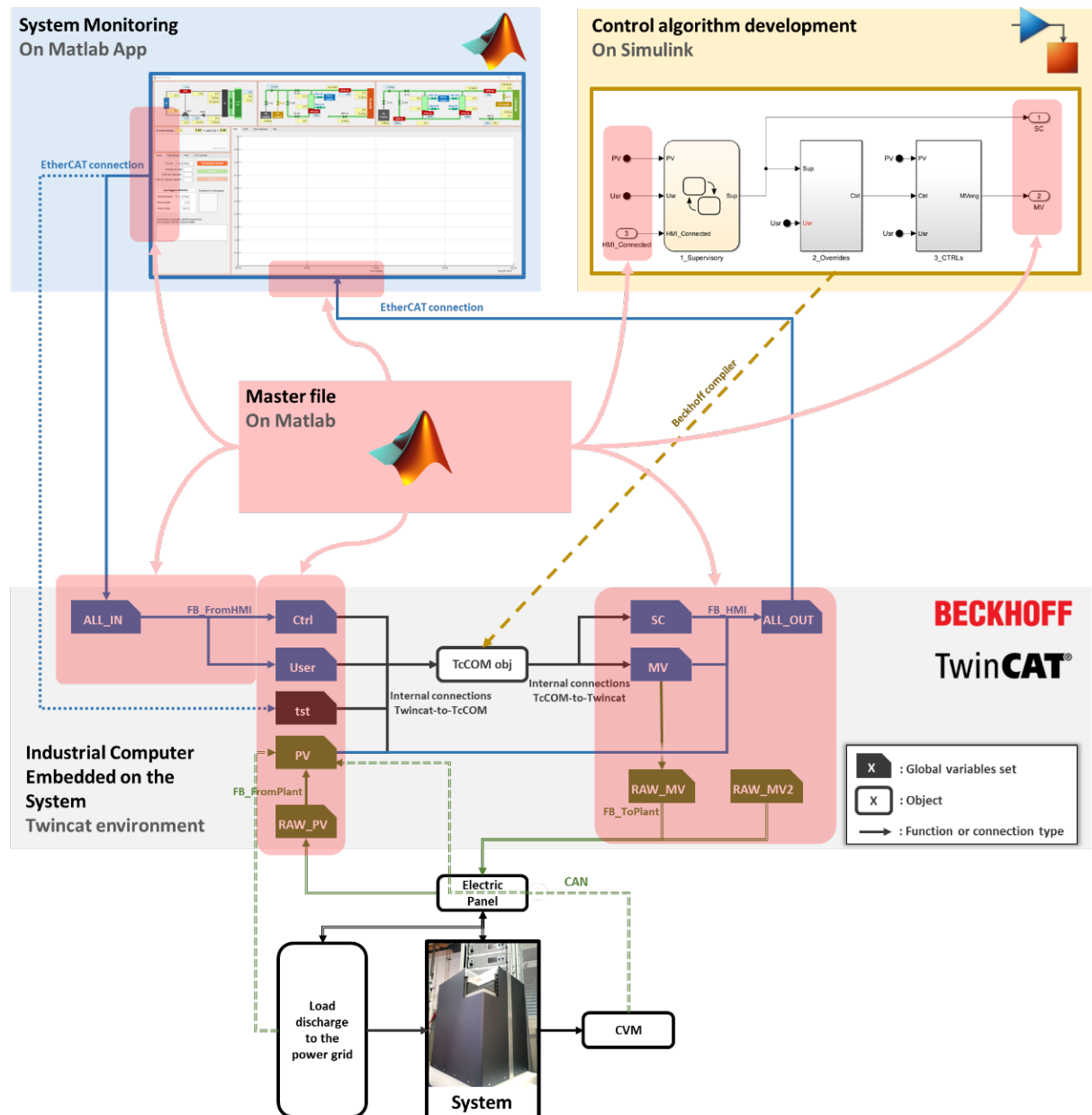
Figure 17. Interconnections between the control modules and how the master file updates them.

2. The industrial computer: an industrial computer from Beckhoff is used for this purpose. It provides all the features mentioned above and is mostly programmed by the master file and a Simulink-to-Twincat compiler. This allows to build the control algorithms on Simulink, a much more convenient and powerful programming software for control. In addition to being the support of those algorithms, this computer

manages the communication between the sensors and actuators of the system and converts all raw signals (voltages) into engineering values (pressures, temperature, etc).

3. The Control Algorithms: The algorithms for the system are developed in Simulink and can be separated into the three components.

1. The Supervisory block contains all the logics which govern what the user is allowed to do in the system.

2. The Override block contains all the tools that are useful for engineers to control the algorithms that are implemented on the system for the first time.

3. The Controller block is divided in five modules: anode, cathode, coolant, high voltage, nitrogen, and each of them contains in-house developed PID controllers.

4. HMI: is designed using MATLAB as a monitoring and driving tool for the user. The layout of the app can be decomposed in three areas depicted on Figure 18.

Area 1. A simplified schematics of the process with indicators corresponding to all the sensors outputs is provided. The user can easily monitor what is happening in the system instantly.

Area 2. All the commands the user can act on are provided this area and four pages are available: the power production, temperatures, the pressures, stoichiometries.

Area 3. All the graphs and tables are placed in this area where three pages are available.

Figure 18. Human-Machine Interface (HMI) of the system.

4 Conclusions

Two types of uniform MPL/GDL layers for PEMFC have been developed and their microstructural properties were investigated. The first type shows comparable properties to conventional materials from existing manufacturer, such as good electrical conductivity, low contact resistance, high porosity, and average thickness. The second type display homogeneously distributed pores and better apparent electrical conductivity, permeability, and diffusivity. Both types of developed layers could perform efficiently and satisfactorily in fuel cells as the reduced size will improve mass transport, reduce ohmic losses, and achieve better water management.

The newly developed methodologies and MPL concept can be expanded further for industrialisation purpose. We have started our initial discussions with a couple of machine producers in Switzerland such as TSE-Coating (https://www.tse-coating.ch/en) for automation and production of thin films with high accuracy.

The concept for small stack up to 15 kW of power has been tested and the configuration of a first prototype has been validated. Experimental tests of several platforms reveal good performances under different operational conditions. The design of 250 kW stack has been developed and the first prototype was built (short stack). Insights into the stack behaviour, such as pressure patterns and temperature homogeneity have been achieved. Performance verifications at larger scales (i.e. 250 kW) is an ongoing activity and will be tested and verified after final manufacturing and testing of the new platform EH-M87 stack.

Modelling integration of the 250 kW stack and system has been accomplished optimising parasitic loads on the BoP components. It results in a more efficient system but also in reducing cost per kilowatt of the entire system, making PEMFC technology more economically competitive.

Overall, simplifying the BoP make fuel cell systems more scalable, allowing for easier integration into various applications and power requirements. This flexibility is essential for adapting PEMFC technology to a wide range of applications, from small-scale portable devices to large stationary power plants. Our application for certification for maritime vessels has been submitted to DNV (det norske veritas) and we have the Approval in Principle. This independent review confirms that the fuel cell design meets all the applicable maritime rules, regulations, codes and standards. Finalisation of the complete Type certification is planned for Q4 2025.

5 Outlook and next steps

The immediate next steps of the project include finalising the procurement of the rest of the components of the system and the test bench, which had previously been delayed due to business constraints in 2023. In parallel, the focus is to improve and produce numerous of the newly developed MPL layers at larger scale and test them in both small and large powered stacks. The final objective will be to integrate the newly developed concept in our stack production machinery that is being currently being designed and assembled our engineering partner's premises in St Gallen before final deployment at our facilities in Nyon.

EHG's key further activities will include a complete assessment of the stack and system in its final configuration (under the conditions in which it will be expected to operate) in order to complete it as a commercialised product. Inherent to this, one of our main objectives is to industrialise the development of this new MPL concept with the assistance of our Swiss partners.

Due to the scale discrepancies in the transport characteristics of the MEA (Membrane Electrode Assembly) and the BPP (pore sizes range goes from micrometres to nanometres), mass transfer for gas permeation and water management is still challenging for fuel cells. We will tackle this with an MPL/GDL with gradient pore size, as it is expected to reduce the effective size discrepancies between the flow channels and the MEA. Another important factor to consider is reduce the interfacial contact resistance. The contact resistance between the BP and GDL is the main source of electrical resistance, which is approximately two orders of magnitude higher than the resistance of the GDL itself. A metal structure of GDL could potentially reduce this resistance but corrosion rate and durability issues would arise consequently. We have already started looking into surface modification of metallic materials to overcome degradation.

Our overall strategy includes a robust plan to expand our market reach and enhance our technological capabilities. We will continue to invest in research and development to ensure that EH Group stacks remain at the forefront of innovation. This involves exploring new materials and manufacturing techniques that could further improve the efficiency and durability of our fuel cells.

EH Group's commercialization pathway is primarily focused on the following markets: stationary power, mining sector, marine and finally aviation. These are all being led by strong regulatory incentives and legislations for those sectors to decarbonize. To that extent we are already commercializing our 40 kW fuel cell systems, as well as our 250 kW module due to be completed this year.

For the stationary power market, our focus is on providing resilient and efficient power solutions for commercial and industrial users where the drivers of decarbonised and decentralised energy systems are driving demand. In the mining sector, we aim to address the critical need for reliable and sustainable power sources in remote, harsh and challenging environments. We already work with major players in the sector who have ambitious decarbonisation targets and see hydrogen as a key vector to meet them.

The marine sector presents both unique challenges and opportunities. We have already received Approval In Principle by certification body DNV for marine applications. This will also enable us to get certification for stationary applications, where the constraints are less strict. Our collaboration with DNV and our participation in H2 Marine (EU funded project) ensures that our fuel cell systems meet stringent maritime regulations and performance standards.

Finally, we are embarking on important collaborations with major global players in the aviation sector to push forward to our technology in that arena. These partnerships are crucial for integrating our fuel cell technology into next-generation aircraft. It will involve multi-year rigorous testing and certification processes to meet the high safety and performance standards required in aviation.

Given that our stack innovation is a platform technology, it also opens up other potential avenues. In particular, our stacks can be operated both as High-Temperature PEM fuel cells and in electrolyser mode. Recent developments in the HT-PEM fuel cells area shows a significant interest from the aviation and marine industry to overcome the challenges of heat dissipation and hydrogen purity. This is an area where can explore the application of our newly developed GDL/MPL concept.

In fuel cells, the GDL, is commonly carbon paper or carbon cloth with an MPL made of a polymer and carbon black. However, in electrolysers, carbon-based substrate and MPL cannot be used due to the corrosive environment of the electrolysers (higher operating voltage). Instead, titanium based GDLs are used. Gas diffusion layers play a vital role in water management and gas bubble removal on electrolysers; hence, optimizing their structure and properties and understanding the methods to achieve this, will help to increase and stabilize the performance of our devices.

Overall, EH Group's approach is comprehensive and strategically aligned with the global needs of decarbonising hard to abate sectors. It addresses the requirements of multiple sectors and working closely with regulatory bodies and industry partners, we are well-positioned to drive forward our innovative stack technology and contribute to a cleaner, and greener future.

6   References

1. Jiao, K., et al., *Designing the next generation of proton-exchange membrane fuel cells.* Nature, 2021. **595**(7867): p. 361-369.
2. Antunes, R.A., et al., *Corrosion of metal bipolar plates for PEM fuel cells: A review.* International Journal of Hydrogen Energy, 2010. **35**(8): p. 3632-3647.
3. Williams, M.V., et al., *Characterization of Gas Diffusion Layers for PEMFC.* Journal of The Electrochemical Society, 2004. **151**(8): p. A1173.
4. Wang, H., M.A. Sweikart, and J.A. Turner, *Stainless steel as bipolar plate material for polymer electrolyte membrane fuel cells.* Journal of Power Sources, 2003. **115**(2): p. 243-251.
5. Forouzanmehr, M., et al., *Detection and Analysis of Corrosion and Contact Resistance Faults of TiN and CrN Coatings on 410 Stainless Steel as Bipolar Plates in PEM Fuel Cells.* Sensors, 2022. **22**(3): p. 750.
6. Guo, Z., C. Zheng, and B. Shi, *Discrete lattice effects on the forcing term in the lattice Boltzmann method.* Physical review E, 2002. **65**(4): p. 046308.
7. Lan, S., et al., *Image recognition of cracks and the effect in the microporous layer of proton exchange membrane fuel cells on performance.* Energy, 2022: p. 126340.
8. Latorrata, S., et al., *Design of properties and performances of innovative gas diffusion media for polymer electrolyte membrane fuel cells.* Progress in Organic Coatings, 2015. **78**: p. 517-525.
9. Tanaka, S. and T. Shudo, *Corrugated mesh flow channel and novel microporous layers for reducing flooding and resistance in gas diffusion layer-less polymer electrolyte fuel cells.* Journal of Power Sources, 2014. **268**: p. 183-193.
10. Shrestha, P., et al., *Graded Microporous Layers for Enhanced Capillary-Driven Liquid Water Removal in Polymer Electrolyte Membrane Fuel Cells.* Advanced Materials Interfaces, 2019. **6**(21): p. 1901157.
11. Chen, Y.-C., et al., *Determination of the porosity and its heterogeneity of fuel cell microporous layers by X-ray tomographic microscopy.* Journal of Power Sources, 2022. **539**: p. 231612.
12. Chen, C.H., et al., *Understanding the Impact of Microporous Layer Cracks on Pt Catalyst Degradation.* ECS Meeting Abstracts, 2022. **MA2022-02**(39): p. 1377.
13. Wang, S., et al., *Enhancing the properties of water and gas management for proton exchange membrane fuel cells via tailored intersected cracks in a microporous layer.* Journal of Power Sources, 2022. **533**: p. 231402.
14. García-Salaberri, P.A., *Effect of Thickness and Outlet Area Fraction of Macroporous Gas Diffusion Layers on Oxygen Transport Resistance in Water Injection Simulations.* Transport in Porous Media, 2022. **145**(2): p. 413-440.
15. El-kharouf, A., et al., *Ex-situ characterisation of gas diffusion layers for proton exchange membrane fuel cells.* Journal of Power Sources, 2012. **218**: p. 393-404.
16. Csoklich, C., et al., *Does the thermal conductivity of gas diffusion layer matter in polymer electrolyte fuel cells?* Journal of Power Sources, 2022. **540**: p. 231539.
17. Kim, K.-H., et al., *The effects of relative humidity on the performances of PEMFC MEAs with various Nafion® ionomer contents.* International Journal of Hydrogen Energy, 2010. **35**(23): p. 13104-13110.

7 Appendix

MPL/GDL Literature review

Year	Paper	Flourinated polymer	Solvent/Surfactant	Protocol Preparation of Gas Diffusion Layer for Fuel Cell.	Instrumental
2009	Park et al.	PVDF + carbon	Acetone/water	Carbon powder was mixed with PVDF in the ultrasonic bath for 2 hours. The obtained carbon slurry was coated onto one side of woven carbon cloth gas diffusion-backing layer by doctor blade method, and successively dried at 80°C for 30 min.	Ultrasonic doctor blade method Temperature. The MPL coated GDL sample was heat treated at 180°C for 1 hours to distribute PVDF homogeneously through the MPL
2013	Tanaka et al.	PTFE + carbon	Distilled water Triton X-100	5:1:20:20 CB:PTFE:surfactant:water	Mixed with 1 mm zirconia beads in a bead mill for 3 h at 400 rpm. Coating was cast onto an expanded PTFE sheet 350 C for 60 min to obtain MPLs 40 mm and 60 mm thick.
2014	Tanaka et al.	PTFE + 1 carbon black or 2 powdered graphite flake or 3 powdered silver flake or 4. stainless-steel foil with golden plating	Distilled water Triton X-100	1. CB:PTFE:surfactant:water 5:1:20:20 2. GF:PTFE:ethanol 5:1:5 3. SF:PTFE:ethanol 5:1:5	1. Mixed with 1 mm zirconia beads in a bead mill for 3 h at 400 rpm. Coating was cast onto an expanded PTFE sheet 350 C for 60 min to obtain MPLs 40 mm and 60 mm thick. 2. hot pressed 3. Hot pressed
2015	Latorrata et al.	Perfluoropolyether PFPE Fluorinated ethylene propylene (FEP) Perfluoroalcoxy (PFA) carbon	Isopropyl IPA Distilled water Triton X-100	Eun-Sook Lee Patent US 2009/0011308 A1 CB was slowly added to a solution of the polymer dispersion and IPA (Triton X-100 in the reference ink preparation based on PTFE [13]) in deionized water. The mixture was vigorously stirred and homogenized by a high shear mixer (UltraTurrax T25) at 8000 rpm for 10 min.	High shear mixer Blade coating technique, using a lab-scale commercial equipment K-101 Control Coater. Temperature (30 min) 150 C PFPE 260 C FEP 305 C PFA
2019	Shrestha et al.	PTFE 10%, 20%, 10-20% carbon	Sonicator Distilled water Triton X-100	The surfactant was added to deionized water in a beaker and stirred under ambient conditions for 15 min using a magnetic stirrer. Carbon black was added to the mixture in three equal batches (by weight), while the mixture was stirred continuously. The mixture was stirred for 10 min after adding each batch. The resulting MPL slurry was stirred for an additional 15 min, and then sonicated for 30 min The PTFE emulsion was added to the slurry, which was mixed for 10 min using a magnetic stirrer and sonicated for 30 min at 50% amplitude in pulse mode (with 5 s on and 1 s off).	Q125 sonicator, Qsonica Sonicators LLC. Adjustable micrometer thin film applicator (Microm II, Paul N. Gardner Company, Inc Temperature 1 hour each: 250 C remove water 270 C remove surfactant 350 C sinter the MPL
2020	Balzaroti et al.	Perfluoropolyether (PFPE) carbon	Isopropyl IPA Distilled water	Eun-Sook Lee patent US 2009/0011308 A1, Carbon black was dispersed into a solution containing distilled water and isopropyl alcohol (Sigma-Aldrich). After the addition of Fluorolink® P56 (Solvay Solexis, Milan, Italy), a perfluoropolyether (PFPE)-based polymer, as hydrophobic agent, the four components were mixed for 10 min at 8000 rpm, by using an UltraTurrax T25 homogenizer (IKA Instruments, Staufen, Germany).	Pre-treated GDLs by using the blade coating technique, using a A K-Control Coater device (RK Print-Coat Instruments Ltd., Litington, UK) Temperature 120C it was found that treating amorphous PFPE-based polymers at a higher temperature would be meaningless